Mariana Parrilha Alexandre Meira
Licenciatura em Ciências Biomédicas

Microfluidics: A New Look at Cell Migration Analysis

Dissertação para obtenção do Grau de Mestre em
Engenharia Biomédica

Orientador: Dr. Abel Oliva, Investigador Principal, ITQB

Co-orientador: Dr. Hugo Águas, Professor, FCT-UNL

Presidente:	Professora Dra. Célia Henriques, FCT-UNL
Arguente:	Professor Dr. Ricardo Franco, FCT-UNL
Vogal:	Dr. Abel Oliva, ITQB

FACULDADE DE CIÊNCIAS E TECNOLOGIA
UNIVERSIDADE NOVA DE LISBOA

Dezembro 2015

Microfuidics: A New Look At Cell Migration Analysis

If we knew what it was we were doing, it would not be called research, would it?

Albert Einstein

Acknowledgments

The development of this project, along with my whole journey until here, would not have been possible – or certainly not so bright – without the support, attention and friendship of some people, to whom I own a sincere *Obrigada.*

At first, to Professor Abel Oliva, my counsellor, for giving me the opportunity to play a part in this project and for all the support provided during this phase. For the tutoring and availability, for the roasting and the laugh.

To Professor Hugo Águas, my co-counsellor, for the opportunity and the reliance. For always being conducive and for showing responsiveness when everything seemed worse.

To the Biomolecular Diagnosis Group, who kindly received me, for lightening up this experience and for always being available. To Carmo, for always being so positive, and for all the guidance and encouragement given along my journey into the *lab*. To Catarina, Mariana, Rita e António, for the countless reasons – for always making me laugh, for the help and advice, for the support and the sharing. To all, for cheering together after the successful assignment and always remembering me of those after the failed ones. To the colleagues across the hallway, for the sympathy and the great doses of humour.

To both the institutions that have made this road possible and always provided the resources needed to its' success – *Universidade Nova de Lisboa & Instituto Tecnologia Química e Biológica António Xavier*. To *CEDOC* (Chronic Diseases Research Centre) and *CEMOP* (Centre of Excellence in Microelectronics Optoelectronics and Processes) for the assets provided and the thankful cooperation shown.

To my friends, both the elderly and the latest. To the first, I need to confess it would never had been possible to get here without you; to Ana, Marina, Sara, Cris, Sérgio and Miguel my dearest regard for always being there even when separated by dozens of kilometres. To the second, for all the growing up together while enjoying it but, mostly, for being a second family in the late years. To who has always been close, for days and nights, goods and bads, a special *thank you.*

At last, to my family for the uncountable support and constant believing. - to my parents, for always encouraging and counselling me to the best - to my sister, for the constant concern and sincere comprehension. To the three, for always making me believe every question has an answer and every problem a solution.

Abstract

This thesis explores the development and employment of microfluidic devices as a tool for studying the effect of the surrounding environment on embryonic stem cells during the migration phenomena. Different single-cell microchips were designed and manufactured to study mouse embryonic fibroblasts (MEFs) migration towards an environmental variation (increase of serum concentration in the culture medium) that was expected to function as a motility stimuli. Considering the experimental, cells were injected into the microchips chambers and individually isolated by dedicated cell traps with view to a single-cell analysis. Once fribroblasts were attached to the surface, culture medium with an increased serum level was subsequently injected in an adjacent chamber to promote the formation of a serum concentration gradient. The gradient established between the chambers could be sensed by the fibroblasts and thus triggered the cells mobilization towards and in the direction of the richer serum medium. Additionally, the experiment allowed the observation of MEFs' structural reorganization when migrating through micro-tunnels containing widths below the cell size, suggesting a cytoskeleton rearrangement on account of the nutritional stimulus introduced. Furthermore, results indicate that fibronectin promotes MEFs adhesion to the substrate and that MEFs migration is characterized as haptotactic.

KEYWORDS: microfluidics, single-cell analysis, MEFs, cell migration, fibronectin

Resumo

O objectivo deste trabalho consiste no desenvolvimento de dispositivos de microfluídica para o estudo do efeito do ambiente extracelular em células embrionárias durante o processo de migração. Neste contexto, foram projectados e fabricados diversos microdispositivos de fluídica com o objectivo de estudar a migração de fibroblastos embrionários murinos (FEMs) perante uma variação extracelular que se previa actuar como um estímulo de motilidade. Em termos experimentais, o processo inicia-se com o aprisionamento das células em estruturas especificamente desenhadas para o estudo *single-cell* numa câmara integrada no dispositivo. Quando as células aprisionadas revelam aderência *relativamente* ao substrato, é inserido na câmara adjacente meio de cultura com um nível superior de soro, de forma a promover a formação de um gradiente de concentração. Foi verificado que o gradiente formado entre as câmaras é sentido pelos fibroblastos e activa a mobilidade celular na direcção de concentração crescente do soro. Adicionalmente, o desenvolvimento do projecto permitiu observar a reorganização estrutural dos FEMs ao atravessar microtúneis de dimensão inferior à sua, sugerindo a ocorrência de fenómenos de reestruturação do citoesqueleto perante o estímulo nutricional induzido. Os resultados obtidos permitiram, ainda, verificar a importância da fibronectina como promotor de adesão celular ao substrato e classificar a migração dos FEM como haptotáctica – devido a variações de composição do meio extracelular envolvente.

Palavras-Chave: microfluídica, análise *single-cell,* FEMs, migração celular, fibronectina

CONTENTS

List of Figures

List of Tables

Abbreviations

Cdc42	Cell Division Control Protein 42
DMEM	Dulbecco's Modified Eagle's Medium
DMSO	Dimethyl Sulfoxide
DPBS	Dulbecco's Phosphate-Buffered Saline
ECM	Extracellular Matrix
FBS	Fetal Bovine Serum
FN	Fibronectin
iPSCs	Induced Pluripotent Stem Cells
LOC	Lab-On-Chip
MEA	Malt Extract Agar
MEFs	Mouse Embryonic Fibroblasts
MRCK	Myotonic Dystrophy Kinase-Related
PDMS	Polydimethylosiloxane
PGMEA	Propylene Glycol Mmethyl Ether Acetate
PS	Pen/Strep
Re	Reynolds number
SCs	Stem Cells
µTAS	Micro-Total Analysis Systems

Chapter 1
INTRODUCTION

1.1. Project Goals

The aim of this project is to develop a platform suitable for tracking and analysing mouse embryonic fibroblasts migration at a single-cell level, i.e., from an individualized perspective. The first challenges that emerged in this context were *"How can we reliably reproduce the cell's environment?", "Can we track them individually for a long period of time?", "Is it possible to create an easily reproductive platform that allows this assessment?".* These questions found answers within the microfluidics' field, so this concept was applied for the development of microminiaturized platforms suitable for the biological essay in mind. The posterior experimental process was established on behalf of fibronectin coated substrates, in order to comparatively visualize and determine the cells response to a specific stimuli - an increase of serum concentration in the culture medium – that is expected to trigger migration.

1.1.1. Motivation

Migration is a central process in several physiological and pathological processes for both simple uni-cellular and complex multi-cellular organisms. Indeed, the orchestrated movement of cells in particular directions to specific locations is a fundamental request for tissue formation during embryonic development and errors in this process can lead to diverse health-related dysfunctions, namely osteoporosis and cancer[1] (Fig.1.1). The past two decades have witnessed great advances in the understanding of the routines underlying cell migration, nonetheless the overall process exhibits so many regulatory steps that it is foreseen that a deeper knowledge can lead to the development of novel therapeutic approaches and applications[2].

Figure 1.1 | Migration in Health Related Processes
Migration stands as central in several physiological and pathological processes. Considering that a cell migration deregulation may lead to serious consequences – osteoporosis, cancer proliferation, among others – a deeper knowledge of factors that regulate migration could lead to the development of novel therapeutic approaches and applications.

With this in mind, seems only natural to develop strategies and explore new approaches in order to deepen our knowledge in this field. Our proposal is to use single-cell analysis as a tool to manipulate and experiment cultured cells to better understand cell migration and respective constraints through motility assays. In this context, a microfluidic platform is used to track Mouse Embryonic Fibroblasts (MEFs), allowing to follow the temporal development of a cell behaviour within a controlled and predictable microenvironment.

Making an allowance for a personal perspective, the possibility to engage this project has been sincerely challenging and academically enriching. Microfluidics presents itself as an area of umpteen possibilities and the development of this assay has allowed me to interconnect engineering and biomedicine, broadening my horizons in the investigation field.

1.2. Cell Line and Relevant Processes

As previously mentioned, the cells chosen to develop this assay were Mouse Embryonic Fibroblasts – MEFs. In this point, a brief characterization and application of these cells is made, as well as a review of the biological phenomena in study, i.e., cell migration.

1.2.1. Fibroblasts

1.2.1.1. Characterization

Fibroblasts are a major constituent of the connective tissue that establish an essential support of all animal tissues – the stroma. Stromal tissue is relatively undifferentiated and stems from the mesoderm layer that synthesizes the extracellular matrix (ECM), reticular fibers and respective proteins, such as collagen and fibronectin[3]. In addition, fibroblasts secrete the ground substance, an amorphous gel-like substance composed of water and specialized molecules that surrounds cells and determines how firm or soft the ECM is. The formation and differentiation of the specialized forms of connective tissue – bone, cartilage, blood and adipose – is, therefore, highly dependent on the composition of the ground substance[4].

Therefore, the main function of fibroblasts is the maintenance of the structural integrity of the connective tissues through the segregation of essential precursors, determining the physical properties of the various connective tissues. Morphologically, fibroblasts are large, flat, elongated (spindle-shaped) cells that grow attached to a substrate. This eukaryotic cells (Fig.1.2) display a remarkable capacity to differentiate and, in an active state, present abundant rough endoplasmic reticulum[5].

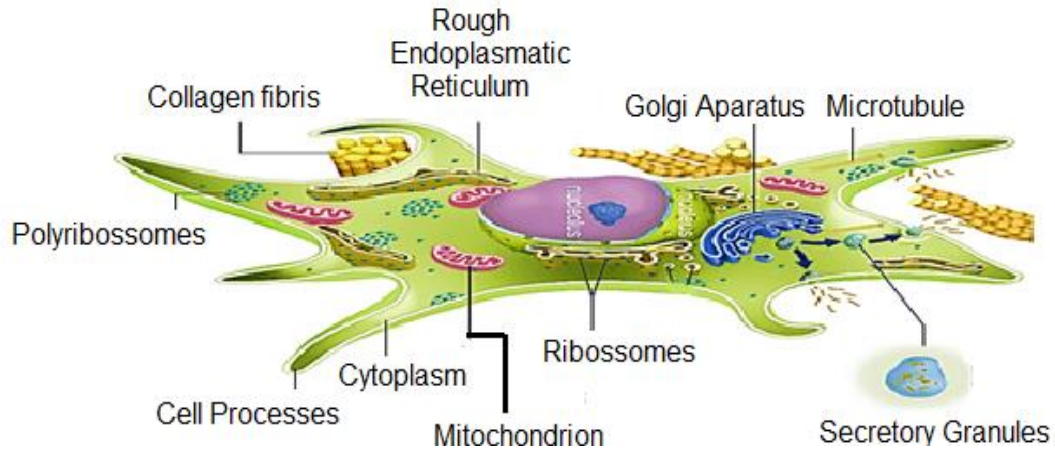

Figure 1.2 | Fibroblast Morphology and Principal Organels

Fibroblasts are the eukaryotic cells responsible for the manufacturing and maintenance of connective tissues, the structural framework supporting the organs of all faunae.[6]

The primary action of fibroblasts is related to wound healing, the process of tissue self-repair after an injury. These specific cells are key players on this response mediation, playing a fundamental role on proliferation, extracellular matrix (ECM) contraction, migration, and ECM production, under the control of growth factors and respective cellular receptors[7,8].

1.2.1.2. MEFs - Secondary Action

This specific cell line is widely used in biotechnological research, essentially due to its' capacity of providing a substrate for stem cells (SCs) to grow in and segregating critical growth factors to maintain SCs pluripotency[9]. Moreover, considerable advances have been made in the embryonic stem cell field as a result of the usage of MEFs, allowing the direct reprogramming of somatic cells to a pluripotent state, i.e., the generation of induced Pluripotent Stem Cells (iPSCs)[10].

In addition, MEFs have been employed in numerous studies related to fibroblast biology, cancer and aging and have also been used to understand several mesodermal cells properties, such as cell cycle regulation, transformation, immortalization, senescence and apoptosis.

Nevertheless, such advances are dependent upon the development of novel approaches in order to understand MEF cells behaviour and structural properties. One of the features that requires particular attention in MEFs' behaviour is their migration ability, essentially because this is a central process within several physiological and pathological processes.

1.1.1. A Glance at Cell Migration

Cell migration is a broad term used to describe the processes involving cells translocation from one location to another. This stands as an evolutionary mechanism that underlies several pathological routines, namely tissue development, functioning and regeneration. Nonetheless, error in this process can lead to severe functional deregulations, such as cancer and osteoporosis[1], pointing out the need and importance of developing new approaches to study this phenomena. It is of general acceptance that the mechanisms implicated in cell migration are often regulated by the same effectors, regardless cell type and model of migration. These mechanisms are coordinated by a complex signalling network – signal and receptors – and include a set of complementing processes comprising polarization, protrusion and adhesion, translocation of the cell body and retraction of the rear [11]. In order to better understand the sequence and portrayal of this complex process, these mechanisms are briefly described along the next sections.

1.1.1.1. Polarity

Within the context of cell migration, polarity describes the functional and molecular differences established between the front and the rear of the cell. Cell polarity is a process reinforced by the environment, a provider of directional cues such as chemotactic (induced by chemoattractants), haptotactic (generated for fluctuations on substrates concentration), mechanotactic (cell-cell contact breakdown), electrotactic (due to electric fields) and durotactic (derived from differences in pliability). The recruitment of specific signalling proteins within the cell is directed by this cues, originating morphological asymmetries characterized by the formation of a defined cell front and rear [12]

Biologically, this process is driven by the actuation of the small GTPase Cell Division Control Protein 42 (Cdc42) through myotonic dystrophy kinase-related (MRCK) in order to control the distance and position of the nucleus with respect to the centrosome (MTOC). Moreover, Cdc42 Division controls partitioning proteins like PAR3 or PAR6 to regulate microtubule dynamics through the dynein/dynactin complex (Fig.1.3)[13].

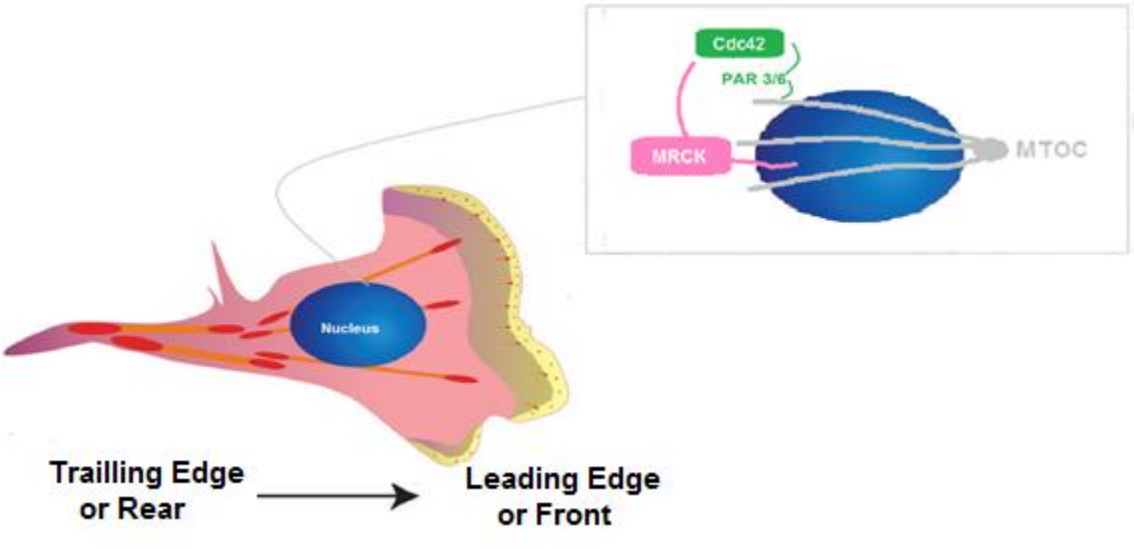

Figure 1.3 | Step One in Migration: Polarity
The major mechanisms involved in cell polarity are the activation of MRCK and PAR3/6, in oder to control the nucleus position towards the MTOC and the microtubule dynamics through the dynein/dynactin complex, respectively. Adapted from [14]**.**

The induction of polarized signals in the course of this event generates the formation of a protrusion at the front of the cell and a rear, also known as leading and trailing-edges. In the specific case of fibroblasts, polarization is thought to be also originated by the myosinII-induced production of stable actin filament bundles and adhesions and consequent cytoskeleton reorganization[15,16].

1.1.1.2. Protrusion

The formation of protrusions comprises a deformation of cellular membranes, a process sustained by the dynamic polymerization of actin cytoskeleton, which consents an expansion in the membrane surface. Actin filaments are essential elements of cell cytoskeletons formed by the polymerization of arrays of monomeric globular G-actin subunits and stand as a physical backbone of a protrusion, determining the cell shape and its internal organization. The self-association of actin filaments into bundles or a branched network is carried by specific actin-binding proteins with cross-linking activity (like α-actinins or myosins) and its' morphology is directly conditioned by them[13].

Throughout fibroblast migration, actin filaments within the cell assume two different morphologies, exhibiting extensions of sheet-like - lamellipodia - or rod-like - filopodia – protrusions. The lamellipodia region is characterized by the formation of a diagonal meshwork of actin filaments and is associated with radial bundles that project filopodia and contractile bundles of actin – the stress fibres (Fig.1.4). The formation of adhesion sites is essential to protrusion, since it provides the necessary traction for the cell stability and adjusts signalling components that regulate actin reorganization and membrane endocytosis[17].

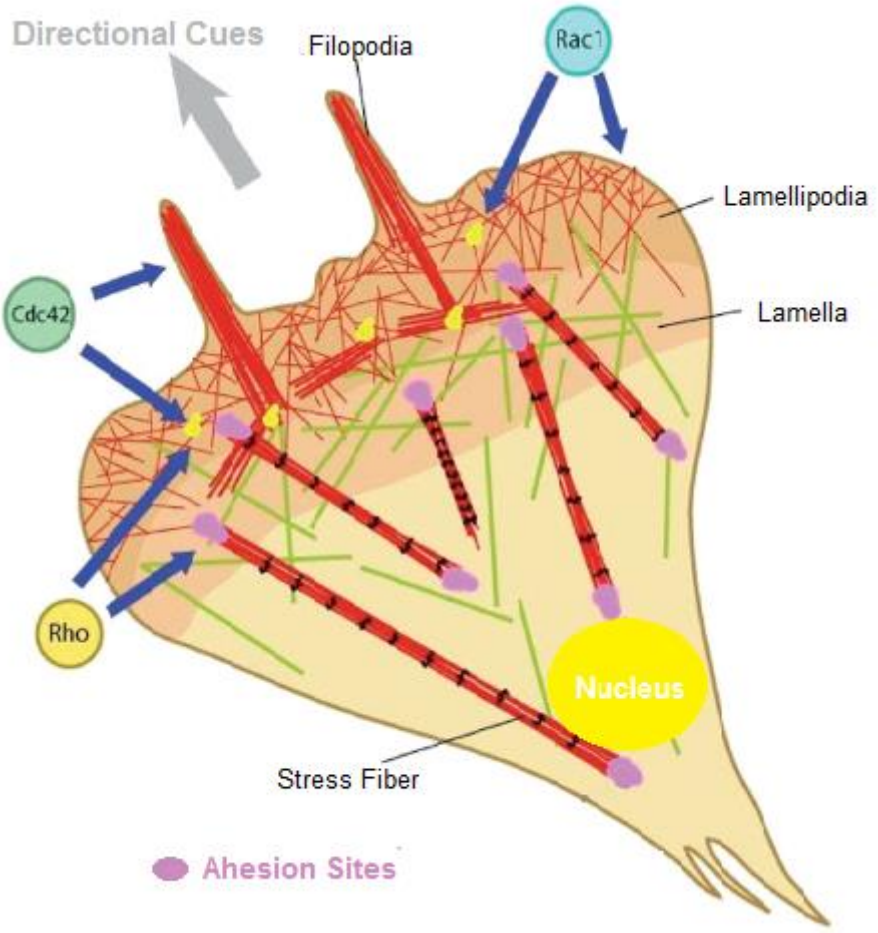

Figure 1.4 | Step 2 in Migration: Protrusion.
The actin cytoskeleton reorganization in a fibroblast protrusion is determined by the formation of lamellipodia (filaments meshwork) and filopodia (association of parallel filaments), as a consequence of actin filaments polymerization. Adhesion sites (marked in purple) are essential in this process, regulating actin reorganization and the cell stability.[17]

1.1.1.3. Adhesion

This mechanism refers to the physical binding of a cell with another cell or with the ECM, under the action of so called cell adhesion molecules - selectins, integrins, and cadherins[18]- after an environmental stimuli. Taking into account the purpose of this project, the focus on this section is the cell-ECM adhesion establishment. On the course of this process, interactions of transmembrane integrins binding to the ECM promote the transduction of the external stimuli that control cell migration into intracellular biochemical signals.

Adhesion is intrinsically coupled with the protrusion development, essentially due to the formation of adhesion sites along the cell during actin polymerization. The cell-ECM adhesion has been widely studied in the past years, allowing the delineation of three major forms of adhesion subclasses evolved in migration, namely nascent adhesions[19], focal complexes[20] and focal adhesions[21]. These structures consist on fundamental sites of convergence between the actin cytoskeleton and ECM fibrils and are closely coupled with lamellipodia and filopodia, the protrusions of the leading edge of the cell (Fig.1.5).

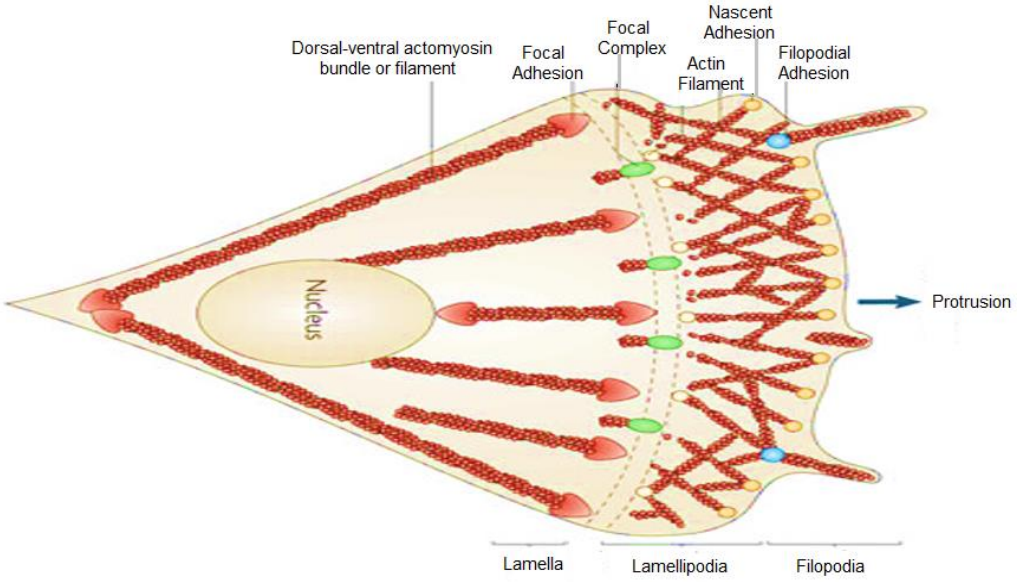

Figure 1.5 | Step Three in Migration: Adhesion
Nascent adhesions are initially formed within lamellipodia and generate signals that activate Rac-1, promoting the formation of focal complexes within the transition zone between lamella and lamellipodia. Focal adhesions are larger structures, comprising a link between the actin cytoskeleton and the ECM. [22]

Nascent adhesions are the first adhesive structures formed, emerging within the lamellipodia. These small dot-like structures reside near the leading edge in protrusions and mediate signals that promote actin polymerization[19]. Since these are highly transient structures, nascent adhesions are not easily identified in some cell types. Focal complexes are also dot-like structures lying at the extreme of the protrusion, which formation is mediated by Rac-1 activation of kinases. On the other hand, focal adhesions are morphologically larger and elongated and are placed at the end of actin filament bundles, both in central and peripheral regions of the migrating cell[22]. These structures are linked to the actin cytoskeleton through the attachment of integrin receptors associated with large complexes of signalling and structural proteins[23], that allow the cell to generate traction and pull its body forward.

1.1.1.4. Retraction

In order to allow the forward translocation of cells, the trailing edge must retract and adhesions at the rear need to be disassembled - otherwise, tension would rip the cell apart. Several mechanisms promote disassembly in cell migrations, including actomyosin contractions, microtubule relaxation and endocytosis of adhesion receptors[2]. In summary, this disassembly process is induced by retraction, a vital force required to move the bulk of the cell forward and complete the migration cycle.

1.3. Microfluidics Technology

Insurgence of Microfluidics

Microfluidics is a multidisciplinary field that has emerged in the beginning of the 1980s as a powerful tool for investigating the inherent complexity of cellular processes. Commonly, microfluidic devices deal with phenomena at a microscopic scale, exhibiting channels with dimensions between ten and hundreds of microns and a volumetric capacity of 100*nl* to 10*µl* [24]. This network of micro-channels is projected together according to the desired function (sort, mix, pump) and is connected to the outside through inputs and outputs pierced through the chip. The injection and removal of liquids or gases is performed using external active systems, such as peristaltic or syringe-pump, pressure controllers or micromixers and a data acquisition system allows to follow the whole process (Fig.1.6).

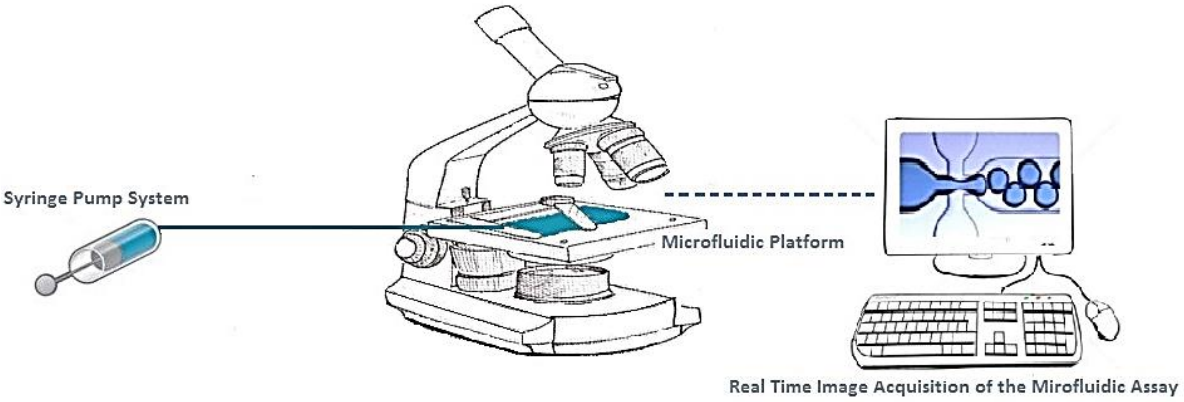

Figure 1.6 | Basic Microfluidic System Setup.
A serynge pump system is used to load the samples through the inlets of the microfluidic device and the phenomena in study is analysed recorring to a real time image acquisition platform.

In order to a get a correct sample analysis in microfluidics, the fluid manipulation within the chip is also of great relevance. The 'pressure driven flow' is a suitable technique often used in this area based in the appliance of pressure in the inlets in order to promote the liquid propagation through the microchannels. Once the sample is placed on the inlet reservoirs, the pressure difference established with the outlets endorses the fluid circulation within the chip. The fluid velocity and flux on the device are ultimately determined by this pressure difference as well as by the fluid's resistance in the microchannels[25]. Considering that fluids behaviour in a microscale has a great influence on this area, this topic is posteriorly analysed in section 1.3.2.

Microfluidics presents a wide range of applications, revolutionizing areas as molecular biology (DNA Analysis and Proteomics), genetic sequencing, clinical pathology, single-cell analysis and the modelling of fluid dynamics. Indeed, the increasing number of microfluidics' publications in journals and conferences from the mid-1990s to today sustains the statement that this is a field with a growing influence in modern science [26]. The advances sustained by this area offer a diverse set of advantages, namely the use of small amounts of reagents and samples, a better temperature control, portability and a high throughput. Further advantages include space for parallelization, faster analysis and waste reduction [27].

The development of microfluidics technology allows the production of devices containing several components with different functions, leading to the idea that one could fit an entire *lab on a chip*. In this context, the global concept of Lab-On-Chip (LOC) or µTAS *(micro-total analysis systems)*

states the scaling down of multiple laboratory processes into a single chip-format (Fig.1.7), allowing the development of scientific studies within a controlled environment and without a formal lab[28].

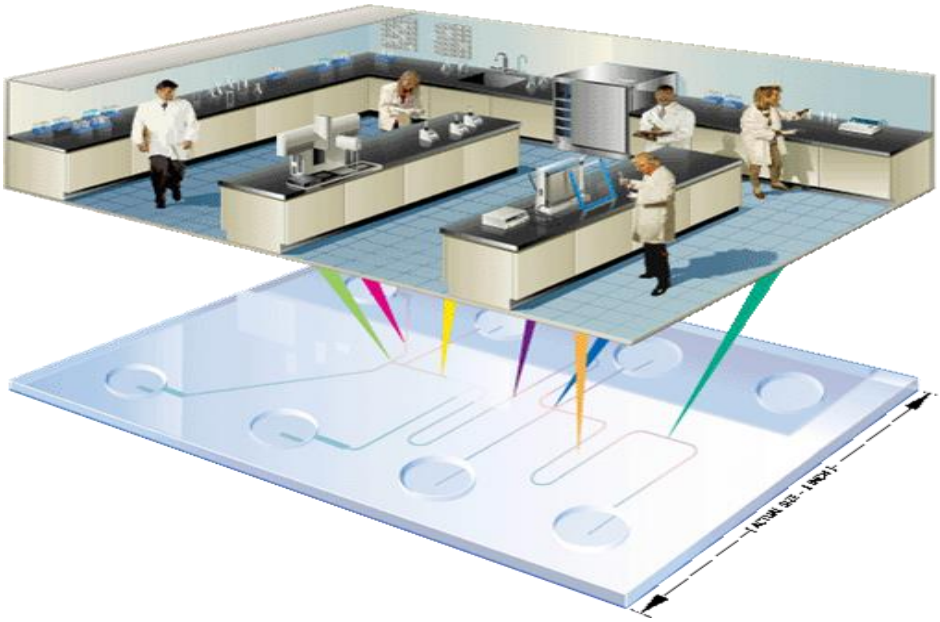

Figure 1.7 | Lab-On-Chip Concept.
LOC designation refers to integration and miniaturization of several laboratory processes on a chip format within a controlled bio-envronment (http://Lab-on-Chip.gene-quantification.info - retrieved in 2015.05).

The next years are likely to be critical in the development of highly integrated microdevices, since the acceptance of microfluidic based technologies in the market will dictate the amount of both private and public funding allocated to this area. Some LOC devices have already been successfully commercialized, in particular a system developed by *Biosite*, that analysis a drop of blood through a functionalized microchannel and determines if a patient has suffered a heart attack[29].

1.3.1. Single-Cell Analysis in Microdevices

Single-cell analyses (SCA) states for the approach of studying cells' behaviour at an individual, and therefore fundamental, level. Cellomics recognise that the way a cell processes input signals decides its particular faith and that individual cells may differ from each other in several aspects. It is likewise defined that a cell dynamics is frequently masked by the bulk response of the average within the same cell type[30]. Moreover, heterogeneous cell response to stimuli is known to occur under identical environment conditions[31], stating the need of a sequential tracking system of single cell dynamics.

Flow cytometry is a technique that allows the quantification of single cell properties within a heterogeneous population, however it reflects the state of the cell at a certain moment in time, presenting merely a snapshot analysis[30]. Making an allowance for the requirement of a temporal development of cells' behaviour and properties, this technique has currently been enhanced by microfluidics methodologies.

Single-cell analysis and microfluidics are nowadays puzzling keywords in the scientific community in order to achieve a better knowledge on the whole range of possible responses of individual cells and their heterogeneity. Considering microfluidic chips exhibit structures in the order of microns, this appears as a quite suitable technology for single-cell manipulation and tracking. With this aim, several strategies have been reported as an attempt to spatially separate and analyse single cells through microfluidics[27]. The use of traps[32], patterns[33], microwell arrays[27,34] and droplets[35] are frequently used techniques in this context (Fig.1.8). Due to the aim and development of the project in development, special attention is dedicated to the first along this thesis.

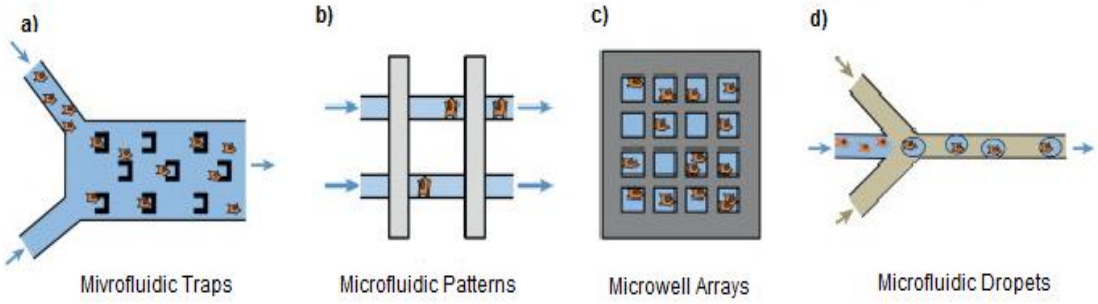

Figure 1.8 | Main techniques used in microfluidic single-cell analysis.
The principal techniques comprising single-cell analysis and microfluidics: a) Microfluidic Traps . b) Microfluidic Patterns . c) Microwell Arrays . d) Microfluidic Droplets. [36]

1.3.2. Fluid Behaviour and Properties in Microfluidics

The fluid behaviour at a microscale is one of the properties that must be taken into account within the microfluidic field. Indeed, fluidic phenomena do not scale linearly from macro to micro implementation, essentially due to the increased surface area-to-volume ratio. Janasek et al. described the main dissimilarities to considerate when working with microfluidic systems, namely the fluids' turbulence – or its' absence: the laminar flow[37]. Undeniably, as the characteristic length in fluidic devices decreases, the inertial forces - that are dominant at a macroscale level - drop significantly compared to the viscous forces. Bearing in mind that inertial forces are the source of turbulence in a fluidic system, the flow regime tends toward laminar at micro dimensions[24]. In this context, the Reynolds number (Re) is a dimensionless parameter of high relevance that expresses the ratio of inertial to viscous forces in studying fluids, according to the equation 1.1.

$$Re = \frac{inertial\ force}{viscous\ force} = \frac{\rho v^2/L}{\mu v/L^2} = \frac{\rho v L}{\mu} \qquad \textbf{Equation (1.1)}$$

where ρ stands for the fluid density; v is the velocity; L is a characteristic dimension (often the smallest length scale of the system, e.g. the smallest width of a channel) and μ is fluid viscosity.

The classification and definition of the various flow regimes was established by Reynolds, through an experiment comprising the injection of coloured water with dissimilar velocities into clear water. The formation of various streak shapes while maintaining the characteristic dimension and the fluid in use, then lead to the establishment of the distinct characterizations - laminar, transitional and turbulent (Fig.1.9):

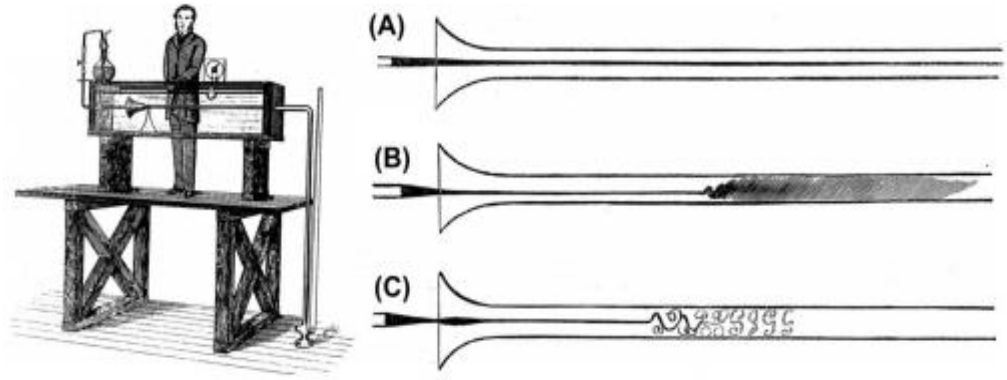

Figure 1.9 | Sketch of Reynolds experiment to determine the various flow regimes.
(A) Laminar flow: smooth, ordered with constant fluid velocity; (B) Transitional flow: intermittent pulses of turbulence; (C) Turbulent flow: disorganised movement with eddy current formation[38].

The transition between laminar and turbulent flow usually occurs for a Re of approximately 2000 (the so called critical Reynolds number), nonetheless this value fluctuates according to the systems' characteristics[39]. In microfluidic systems, the Re is usually below 1, essentially due to the low characteristic dimension values of the devices.

Contrarily to large scales, at a microfluidic level fluids do not mix connectively, i.e., when two fluidic streams come together in a microchannel they flow in parallel, without turbulence, and mixing only occurs as a result of molecules diffusion between the fluids[24]. Therefore, the mass transport takes place only in the direction of the fluid, which is an important characteristic when developing fluidic experiments. In one dimension, the diffusion process can be modelled according to the equation 1.2.

$$d^2 = 2Dt \quad \textbf{Equation (2.2)}$$

where d is the mean distance that a particle travels, D is the diffusion constant and t is the time.

1.3.3. Microfabrication

Microfabrication refers to the process of manufacturing systems with micrometric features, namely microfluidic platforms. This platforms fabrication can be accomplished through several methods, such as photolithography[40], replica molding[41], micro contact printing[42], micro machining[43], and hot embossing[44]. It must be taken into account that microchips production is primarily based in lithography, a fabrication technique well-established in the field of Integrated Circuit technology (Fig.1.10). This method allows the obtention of a direct replica of a plastic, glass or silicon wafer and can be repeated several times for obtaining a functional micro-device[45].

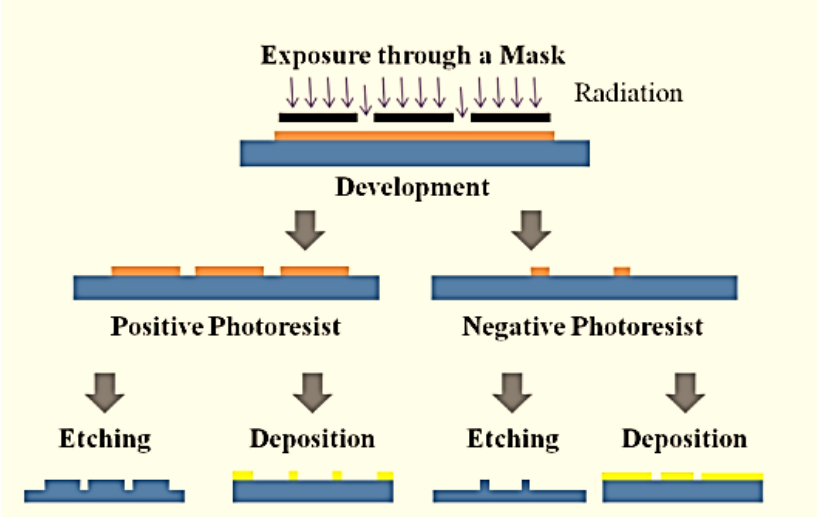

Figure 1.10 | Lithography: sketch of a standard microfabrication process.
This technique consists on the obtention of a direct replica of the original mask (positive resist) or its' inverse (negative resist), prior to exposure and development. In due course, deposition and etching can be performed through addition and subtraction to achieve the desired pattern.

Subsequently, a substrate is spin-coated with a layer of a photoresist – a high sensitive polymeric film. In the second step, the resist is exposed to radiation through a mask and it is observed that the exposed regions change their solubility towards an appropriate solvent called developer. After the development, the exposed pattern is released and the resulting structure can be the final one or be transferred to the substrate by addition or etching processes.

Photoresists are photosensitive polymeric materials commonly used to form a patterned coating on a surface. The development of such advanced materials have allowed the reduction of lithographic structures down to sub-100*nm* dimensions[46]. Photoresists can be either positive or negative, a fundamental property defined as tone. When a negative photoresist is used, the coated region remains insoluble to the developer once it is exposed to radiation and the unexposed one becomes soluble. On the other hand, treatment with a positive photoresist conducts to the solubility of exposed areas and consequent insolubility of the unexposed. According to the microelectromechanical systems industry, photoresists' relevant characteristics differ according to its' tone (Table 1.1). Examples of photoresists regularly used in microfluidic device fabrication include negative toned SU-8 or P-50100 and, as a positive variant, the novolac resin SPR 220-7[45].

Table 1.1 | Relevant photoresists' characteristics according to the respective tone.
Photoresists' characteristics relevant in the microfluidic device fabrication device, according to the microelectromechanical systems industry[45].

Characteristic	Negative Photoresist	Positive Photoresist
Relative Cost	Less Expensive	More Expensive
Step Coverage	Lower	Higher
Developer Base	Organic	Aqueous
Minimum Feature	2 µm	0.5 µm and below
Adhesion to Silicone	Excellent	Fair
Wet Chemical Resistance	Excellent	Fair

Regarding the materials, silicon and glass were the prime options explored in this area, mainly due to their known reputation in the semi-conductor industry. In the late years, novel materials have been introduced to the field, essentially with the purpose of manufacturing simplification and respective cost reduction[47]. In this context, polymers suitable for soft lithography gained special attention, in particular elastomeric polymer poly-dimethylsiloxane (PDMS). In addition to the lower production costs, PDMS is a soft polymer with attractive chemical and physical properties, such as elasticity, optical transparency, low permeability to water and low electrical conductivity. Ultimately, the use of an elastomeric polymer moulding during soft lithography allows the rapid prototyping of microchips, discarding the need of re-using microchips and contributing to a decrease of contamination between assays[48]. Nevertheless, PDMS based micro-devices may present a few disadvantages, namely the possibility of features' shrinking or sagging during microfabrication and the incapability with some organic solvents[47].

The access to the different fabrication materials and techniques makes it possible to project several microchips with specific features like biological or chemical compatibility, faster prototyping or lower production costs, etc. The final choices always depend on the aimed application of the device in use.

Chapter 2
Materials And Methods

2.1. Biological Samples

As previously mentioned, Mouse Embryonic Fibroblast (MEF) was the cell line used in the course of this project. MEF cells – a kind gift from CEDOC (Chronic Diseases Research Centre) - were cultured and arranged to the assays according to that institution´s protocol, as described in this section. This process comprises the cell growth within the appropriate conditions and the post-treatment to suit the migration experiments. In this context, cells were mitotically inactivated (to prevent the nucleus division during the biological assays) and coated with fibronectin (FN, a protein that shall promote migration). The biological samples were then adopted to growth medium with a serum concentration of 1% (v/v) and applied to a microfluidic system in order to reproduce a migration process. A schematic representation of the biological samples acquisition is displayed below, in Figure 2.1.

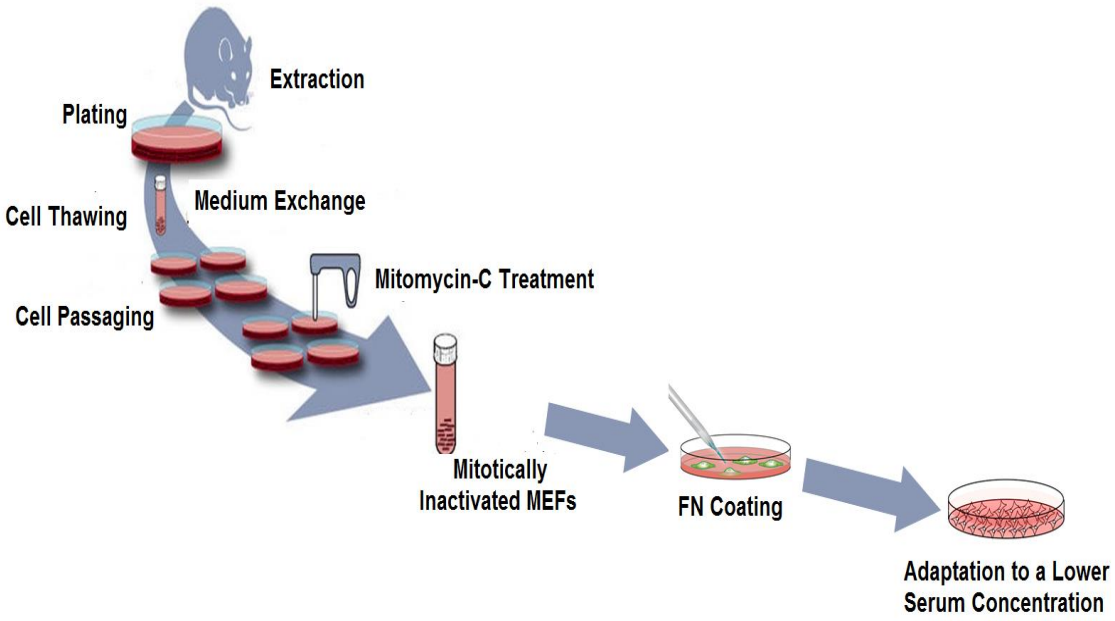

Figure 2.1 | Schematic representation of the steps comprised in the cell line development
After the murine extraction, the cells were plated and thawed in a sterile environment. Cell medium was exchanged every 2 days and the MEFs were passed at specific confluency and concentration levels. Afterwards, the cells were mitotically inactivated, coated with fibronectin (FN) and adapted to growth in a medium with lower serum concentration.

In order to preserve the integrity of the cells and according to cell culture fundamentals, all the routines described within the cell handling were proceeded in a laminar air flow (LAF) chamber, until the moment they were introduced in the chips. The development of the cell line was handled with resource to ITQB facilities and through the tuition of the Biomolecular Diagnosis Team.

2.1.1. Cell Line and Culture Media

Thawing the Cells

MEF cells had been previously frozen at 1×10^6 $cells/mL$, 1mL per vial. These cells were transferred to a centrifugation tube and resuspended in 4mL of growth medium at 37^oC. Culture medium was prepared with 89% (v/v) DMEM medium (Dulbecco's Modified Eagle's Medium,

Sigma Life Science) and supplemented with 10% (v/v) FBS (Fetal Bovine Serum, Lonza) and 1% (v/v) PS (Pen/Strep, Gibco). Cells were pelleted by centrifugation (1100*rpm*, 7*min*, 4*ºC* @ Biofuge 28RS) and, after supernatant removal, resuspended in the medium in a final volume of 6mL. After transferring the suspension culture into a 6*cm* dish shaker flasks, it was placed on an incubator at 37*ºC* in a humidified atmosphere containing 5% CO_2.

Medium Exchange

Medium was replaced by removing the remaining in culture and adding 6*mL* of fresh growth medium at 37*ºC*. The cell culture was then transferred into the incubator again. Culture medium was replaced every 2 days until growth and confluence became evident.

Passaging the Cells

Cell passaging was conducted once cell confluency achieved a level of 60% to 70% and at a cell concentration of approximately $1 \times 10^6\ cells/mL$ *. After culture medium removal, MEF cells were washed twice with DPBS (Dulbecco's Phosphate-Buffered Saline, Gibco) and trypsinized with 1*mL* of a 1x Trypsin-EDTA solution (Gibco). The culture was then transferred into the 37*ºC*, 5% CO_2 for a period of approximately 7 minutes, to promote the actuation of trypsin. The trypsinization process was interrupted by the addition of 6*mL* of pre-warmed fresh medium [cell de-attachment is completed once turbidity is observed in the solution]. Cells were then transferred to a centrifugation tube, pelleted (1100*rpm*, 7*min*, 4ºC) and re-suspended in 6mL of fresh medium. The final solution was aliquot in three vials with 2mL, each containing an approximate concentration of $1 \times 10^6\ cells/mL$. One of the aliquots was transferred to a new culture dish and kept for further passaging in the incubator with a supplement of 4mL of fresh growth medium. The remaining aliquots were centrifuged (1100*rpm*, 7*min*, 4*ºC*) and, after supernatant removal, resuspended in 1*mL* of cryopreservant – 20% (v/v) FBS, 70% (v/v) DMEM, 10% (v/v) DMSO (Sigma). Cells were then placed in cryopreservation tubes and kept in liquid nitrogen as a resource to a future prospect of recreating the same experiments with the descendants through posterior passaging.

* The obtention of growth profiles allowing the determination of the cell concentration are broadly described below, as it is a relevant procedure included in the cell line establishment.

*Cell Concentration Determination

Growth profiles were acquired through monitoring cell concentration and correspondent viability every 48*h.* These parameters were obtained with the trypan blue exclusion method through a 0.1% (v/v) solution with DPBS, with a dilution factor of 5. Cell count was proceeded in a haemocytometer (0.100 *nm*, 0.0400 mm^2OptikLabor) on an inverted microscope (Nikon Eclipse TE 2000-5) with an aim of a $1 \times 10^6\ cells/mL$ concentration. This process was implemented according to the rule on Fig.2.2., expressing that during the haemocytometer reading, the cells attached to the top and left sides of each square were included in the counting whereas the ones at the bottom and right ones were not considered.

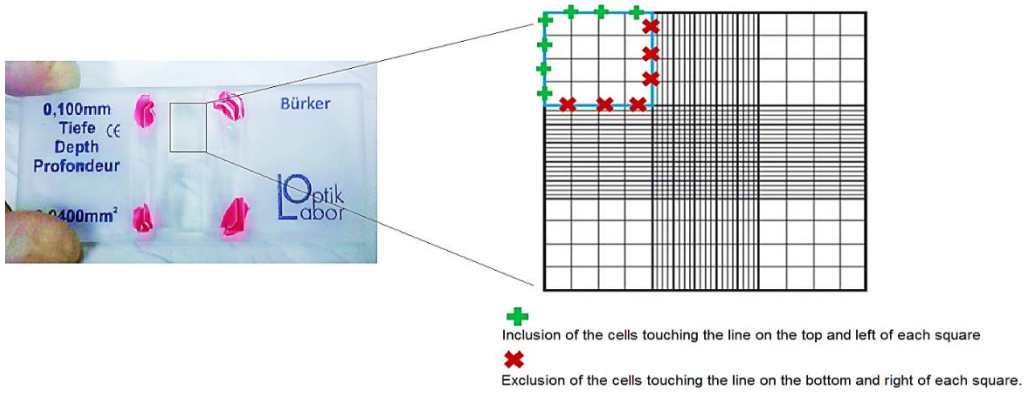

Figure 2.2 | Haemocytometer used to determine cell concentration and correspondent reading method.
In this project, the cells located on the haemocytometer lines marked in green were included in the counting whereas the ones marked on red were discarded.

2.1.2. Adaptation of the Cell Line for the Experiment

Mitotic Inactivation

Cell medium was replaced by the addition of 6*mL* of fresh medium containing 1.5 $\frac{\mu g}{mL}$ containing mitomycin-C (Sigma, 0.5 $\frac{mg}{mL}$ stock). The culture was then incubated for approximately two hours at 37*ºC* in an atmosphere containing 5% CO_2. Afterwards, the medium was removed and the plate containing the adherent culture was washed three times with fresh medium to remove all the existent mitomycin. To prepare the cells for the subsequent steps, additional 6mL of fresh growth medium was added to the plate. When handling mitomycin-C one must consider that this is a genotoxic substance and must be manipulated with reinforced gloves and disposed according to the house rules for these materials.

Adjustment to Lower Serum Concentration

In order to verify if a variation in the medium composition would act as a trigger towards cells motility, the culture was submitted to a starvation period. So that, MEFs were temporarily fed with fresh medium containing 98% (v/v) of DMEM and supplemented with 1% (v/v) FBS and 1% (v/v) PS. The starvation was proceeded right before the experiment, during the trypsinization

2.2. Non-Biological Samples

Along this section, the processes preceding and including the microdevices' fabrication are described according to the procedures adopted to develop this project. In a summary, this process was initiated with the design of the microfluidic patterns and correspondent modelling and optimization. Furtherly, the chips were fabricated in a temperature controlled clean room, according to the stated specifications, and integrated in the migration assay.

2.2.1. Chip Design and Performance Simulations

AutoCAD design of microfluidic devices

The process of microfluidic devices' fabrication requires a prior stage of design and simulation, consistent with the specific aim of the experiment in development. In this context, AutoCAD Software (2015) was used to project the mask comprising the microdevices employed in the migration studies. This software is widely used for engineering layout of geometric features, allowing a high degree of detail, organization, complexity and replication[49]. This aspects make it a very useful tool for low-cost photolithographic processing, conventional in the microfluidic field.

The suitable designs were developed in order to allow single-cell trapping and quantification, forecasting the need of a chemical gradient formation within the chip. The micro-structures were designed taking into account the MEF cells' dimensions, containing at least two inlets for the injection of the medium containing the different serum levels.

COMSOL Multiphysics Simulations

COMSOL Multiphysics is a software based on advanced numerical methods used for modelling and simulating diverse physical phenomena. This platform was exploited with the purpose of optimizing the microchips and respective structures in a process comprising several variations of the experimental parameters (traps' dimensions and distribution, fluid initial velocity, relative pressures) and consequent re-design.

Considering the purpose of the microfluidic devices projected, the modelling was done through studies of fluid characterization, particle tracing and transport of diluted species. All of the simulations were performed at a two dimensional level and the structural material was defined as PDMS, with water as the fluid flowing through the microchannels. The modelling ultimately allowed the determination of the final microfluidic' structures, according to the specifications of the migration assay projected – formation of a chemical gradient, single-cell trapping and a suitable environment to promote migration.

As a result of the previously mentioned processes, a Chrome Soda-Lime mask containing the specific designing of the fluidic devices is projected (Fig.2.3) and posteriorly manufactured by a service provider company (JD Photo-tools, UK)[50]. This mask was then used in our microfabrication process (Section 2.2.2.) to optically project the patterning in a silicon wafer, the primer structure of the micro-devices. In view of Fig.2.3, the radiation will be blocked through the black regions and pass within the white ones into the silicon wafer coated with the negative photoresist SU-8.

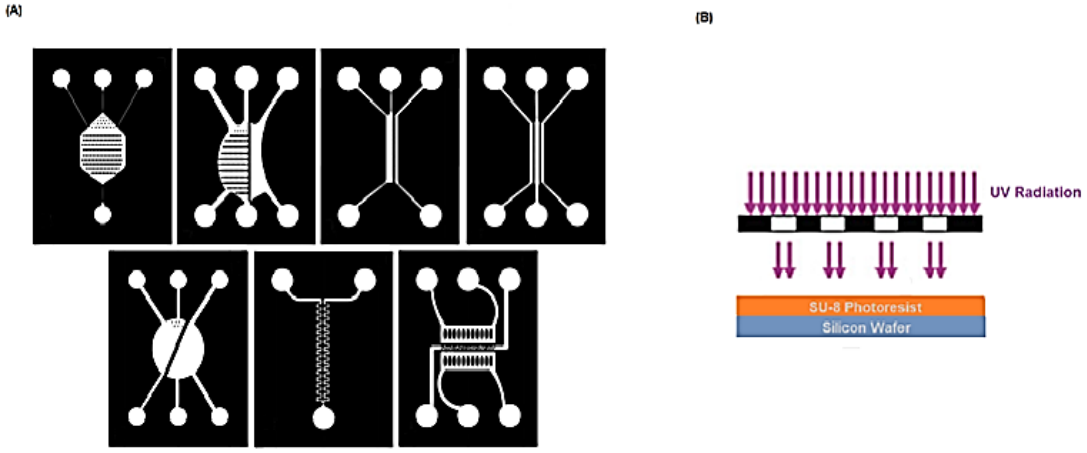

Figure 2.3 | Plot of the specific mask (A) used to optically obtain the chip's patterning through the exposure to Ultra-Violet Radiation (B).
(A): Display of the mask with the microfluidic devices´ structures imprinted, in a total of six chips. (B): Application of the mask in the posterior microfabrication process, according to the chosen photoresist.

2.2.2. Microfluidic Platform

The chips used in the assays were obtained through a lithography-based process, according to the priorly obtained chromium mask. PDMS was the material chosen to manufacture the devices, with SU-8 as the photoresist used to coat the substrate. Microfabrication comprises a sequence of slightly complex procedures, which parameters must be adapted according to the specifications of the biological assay in course. The devices were manufactured with resource to the CEMOP (Centre of Excellence in Microelectronics Optoelectronics and Processes) facilities and under the considerate guidance of the investigator Catarina Freitas.

2.2.2.1. Wafer Preparation

The microfabrication process starts with a pre-treatment of the substrate, the silicon wafers that supplement the SU-8 deposition. At first, the wafer is cleaned with acetone and isopropanol and submitted to ultrasounds for a period of 10*minutes*. Posteriorly, it is baked at 180*ºC* for 10*minutes* – to promote the removal of the adsorbed water molecules – and left to cool down for approximately 10*minutes*.

2.2.2.2. SU-8 Processing

The processing of SU-8 is the most critical procedure in the microfabrication process, essentially because this material properties are greatly affected by parameters variations [46]. This procedure comprises a set of five sequential routines, including the coating, soft baking, exposure, post baking and development (Fig.2.4). Taking into account the dimensions of a single MEF cell, the aimed channel depth of the chips was of ≈ 80*μm*, which is a parameter of great relevance in the whole processing of S8-8. Indeed, the height of the SU-8 layer is defined by the different variables included in this process, standing out the relevance of this mechanism.

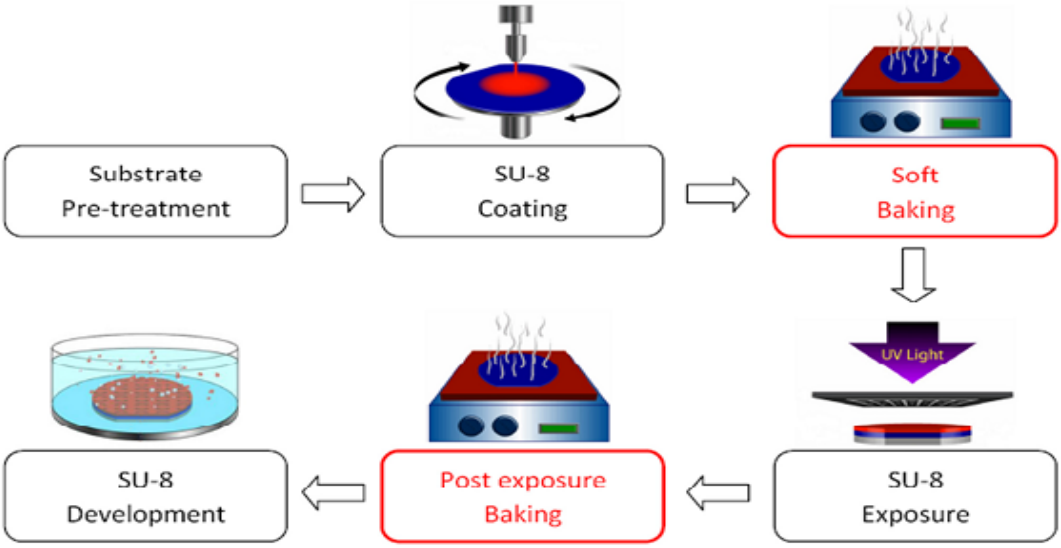

Figure 2.4 | Representation of the sequential procedures of the SU-8 master fabrication.
After the substrate pre-treatment, the samples were submitted to spin-coating and soft baked to promote the solvent evaporation. The samples were then UV irradiated to initiate the cross-linking, that is enhanced during the post bake. At last, a developer bath was prepared and the unexposed regions of SU-8 are removed within the solution. [51]

Spin-coating is the first step of microfabrication and the spin speed was set at a known room temperature, according to the Datasheet on Fig.2.5. One must considerate that these values are stated for a room temperature of 21*ºC* and that a variation of 1*ºC* implicates a readjustment in the order of 25*rpm* in the spinning speed. This rearrangement was set due to the fact that SU-8 viscosity decreases with temperature, hence the speed should be reduced 25*rpm* for a temperature increase of 1*ºC* and contrariwise.

Therefore, after pouring 4mL of 2050 SU-8 in the wafer (10*cm* diameter), the sample was submitted to spin-coating at 21.0*ºC* during 7*seconds* with a speed of 1850*rpm* and 300 $^{rpm}/_{s}$ of acceleration. In order to optimize the procedure and obtain the specified height, the primary experiments included three trials with a deviation of 100 *rpm*, i.e., 1700*rpm*, 1800*rpm*, 1900*rpm*, leading to the mentioned value above.

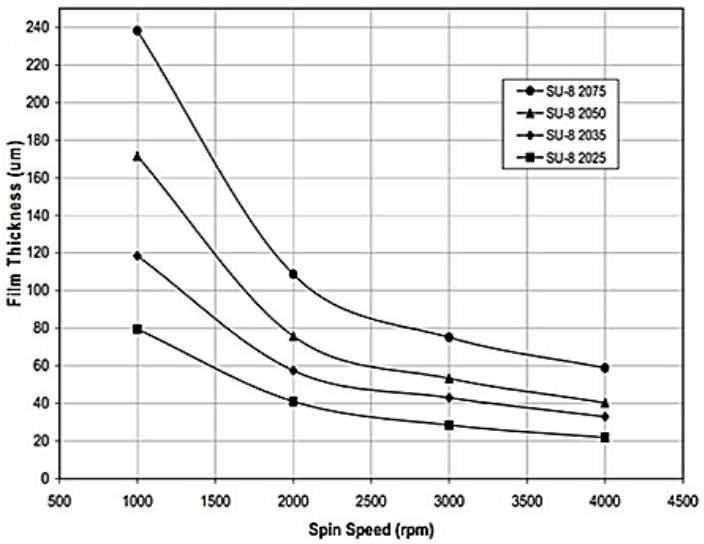

Figure 2.5 | Datasheet Representation of the spin coating speeds according to the fil thickness.
The values presented are stated for a room temperature of 21ºC and must be adjusted according to the real temperature: a deviation in 1ºC implies a variation of 25 rpm in the spinning speed. Adapted from [52].

Posteriorly to the spin-coating process, the wafer was soft baked in the course of two stages in order to promote the evaporation of the solvent. The wafer was placed on a levelled hot plate at 65°*C* during 4 minutes and then transferred to another hot plate at 95°*C* for 8*min*. Once again, these parameters are dependent upon the desired thickness of the final chip and must, therefore, be readjusted towards a different constraint (Table 2.1). The baking time was optimized by keeping the wafer a few additional minutes at 95*ºC* if wrinkles would appear after cooling down.

Table 2.1 | Datasheet for the soft bake duration acording to the desired film thickness.
The soft baking time was defined considering the thickness of the final chip in a two phases sequential process – at first for 65*ºC* and formerly for 95*ºC*. Adapted from[52].

Film Thickness (*μm*)	Soft Baking Duration (min.)	
	(65*ºC*)	(95*ºC*)
25 – 45	0 – 3	5 - 6
45 – 85	3 – 5	6 – 9
85 – 115	5	10 – 20
115 – 160	5	20 – 30
160 – 225	7	30 – 45

After the wafer has cooled down and SU-8 deposition was completed, the sample was UV exposed in a mask aligner (MA6, Suss MicroTec, Germany). The exposition was proceeded by submitting the wafer to UV radiation of approximately 400nm, through the chromium mask with the chip structure imprinted. The exposure energy applied was chosen according to the SU-8 datasheet specifications (Table 2.2) and the time of exposition determined by means of the Equation 2.1, considering a power density of 18.4 $\frac{mW}{cm^2}$. As a result, the UV exposure parameters were set for an energy of 200 $\frac{mJ}{cm^2}$ in a period of 11 seconds, allowing the demarcation of the mask – and respective microfluidic structures - within the SU-8 in the wafer.

Table 2.2 | Datasheet for the exposure energy acording to the desired film thickness.
The exposure dose was chose as a function of the thickness of the micro-chip, allowing the determination of the UV exposition time. Adapted from [52].

Film Thickness (*μm*)	Exposure Energy ($^{mJ}/_{cm^2}$)
25 – 45	150 – 160
45 – 85	150 – 215
85 – 115	215 – 240
115 – 160	240 – 260
160 – 225	260 - 350

$$Exposure\ Time\ (s) = \frac{Dose\ \left(\frac{mJ}{cm^2}\right)}{Power\ Density\ \left(\frac{mW}{cm^2}\right)} = \frac{200\ \left(\frac{mJ}{cm^2}\right)}{18.4\ \left(\frac{mW}{cm^2}\right)} \approx 11s \qquad \textbf{Equation (2.3.)}$$

As soon as the the exposure was completed, the wafer was submited to a post bake bound for completing the cross-linking process. This procedure comprises two heating phases – 65ºC and 95ºC -, for a period of, respectively 2 minutes and 7.5 minutes (Table 2.3). It is important to notice when the micro-pattern becomes evident by naked eye, which should happen between 5 to 15 seconds after plating at 95ºC. Otherwise, one should readjust the exposition dose considering that a shorter time may be a consequence of a higher than recommended dose of UV, and contrariwise for a longer time.

Table 2.3 | Datasheet for the post bake duration acording to the desired film thickness.
The post baking time was defined considering the thickness of the final chip in a two phases sequential process – at first for 65ºC and formerly for 95ºC. Adapted from[52].

Film Thickness (*µm*)	Post Baking Duration (min.)	
	(65ºC)	(95ºC)
25 – 45	1	5 - 6
45 – 85	1 - 2	6 – 9
85 – 115	2 – 5	10 – 20
115 – 160	5	20 – 30
160 – 225	5	30 – 45

To conclude the SU-8 Processing, a developer was used to chemically dissolve the unexposed regions covered by the photoresist. The wafer was developed in constant magnetic agitation at 500 rpm by means of propylene glycol methyl ether acetate (PGMEA) for approximately 7 minutes, according to the specifications on Table 2.4. Subsequently, it was rinsed in clean developer and then washed with isopropanol for another 10 seconds with strong manual agitation. At last, the wafer was gently dried with compressed nitrogen and the existence of white traces in its surface was evaluated. If white traces would appear the sample was developed in a fresh agent for an additional minute and rinsed, until no traces were evident in the wafer. At last, the wafer was observed by optical microscopy to verify if the development time was appropriated, considering that peeling of the SU-8 may occur if the development exposure time is too high.

Table 2.4 | Datasheet for the development time acording to the desired film thickness.
The development process is essential to promote the dissolution of the unexposed regions of the wafer and the obtention of the design structures. The time of actuation of the developer was established considering the desired thickness Adapted from[52].

Film Thickness (*µm*)	Development Time (minutes)
25 – 45	4 – 5
45 – 80	5 – 7
80 – 115	7 – 10
115 – 160	10 – 15
160 – 225	15 - 17

2.2.2.3. Casting of PDMS mould

The casting of the PDMS mould consists in obtaining an intermediate replica of the original SU-8 master made of PDMS. Subsequently, a new replica can be casted from the PDMS mould – an epoxy mould – and the final PDMS chips are then acquired. Even though the chips could be directly casted from the SU-8 master, this intermediate process was chosen because the master has a tendency to peel and thus the process was optimized in a long term perspective.

A 35g solution of PDMS (Sylgard 184, Dow Corning, Spain) was prepared by mixing a curing agent and a base in a 10:1 weight ratio. The sample was then mixture and transferred to a vacuum desiccator for 1 hour, to facilitate the degasification of the bubbles formed. Simultaneously, the SU-8 master was placed in a Petri dish covered with acetate foil and also desiccated during 1 hour. Subsequently, the PDMS was poured over the SU-8 mould, and the sample was desiccated and thermally cured. The curing was performed on a levelled hot plate at 65ºC for approximately 3h30. Ultimately, the cured PDMS was peeled from the S8-8 master by cutting and gently pulling the layer formed upon the wafer (Fig 2.6).

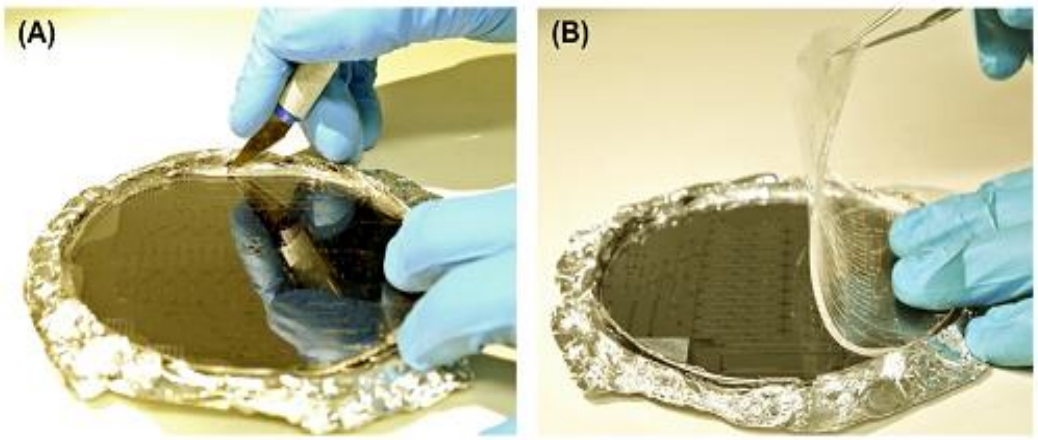

Figure 2.6 | Photographs of the steps used to cast the PDMS and obtain a replica of the SU-8 master mould during the chips fabrication.
(A): A PDMS solution containing a current agent was poured onto the SU-8 master and cured. (B): After the curing, the PDMS replica was peeled of the master by cutting and gently pulling the polymer layer.

2.2.2.4. Casting of Epoxy mould

As previously stated, a processing technique using epoxy as an intermediate mould was included in the fabrication process. This resolution was made considering that epoxy is a much more robust material (due to its monolithic structure) than SU-8, which has a tendency to peel after a few processing.

The PDMS cured mould was placed on a Petri dish with the negative relief features up and an epoxy resin was poured upon it to form a thick layer of approximately 2 mm. Afterwards, the sample was desiccated for 72 hours and cured in a levelled oven at 120ºC for 40 minutes. The ultimate epoxy mould was then obtained by peeling from the PDMS. It is important to reveal that the baking time may vary a few minutes, thus one must verify a small change in colour from white to light yellow to be certain that the mould is prepared.

2.2.2.5. Casting of PDMS chips

At last, the final PDMS chips were casted from the epoxy mould through soft-litography, in a procedure similar to the described for the obtention of the first PDMS mould (Sections 2.2.2.3 to 2.3.3.). The inlets and outlets were then obtained by piercing the PDMS with a blunt needle. The microfabrication procedures used in this experiment are resumed in Fig.2.7, through a display of the samples obtained in each step.

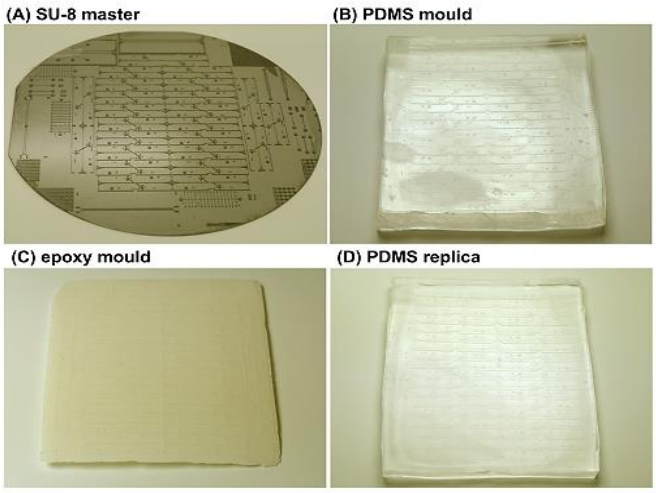

Figure 2.7 | Samples obtained in each step of microfabrication - a summary of the process.
The process was initiated with the fabrication of a SU-8 master (A) and, subsequently, a PDMS mould was casted once (B) to obtain a mould suitable for patterning of an intermediate epoxy mould (C). The epoxy mould was then used to produce several PDMS replicas containing the final chips (D).

2.2.2.6. Sealing of PDMS chips

The last step of microfabrication comprises the irreversible sealing of the PDMS chips, a process required to prevent fluid leakage during the experimental assays. The final chips were bonded by oxygen plasma at 100W during 60 seconds in 13*Pa* (Plasma electronic Buck Technologien, Germany) to glass slides – Fig.2.8. Afterwards, the microchips were put into contact with glass and submitted to baking in a hot plate for 15 minutes at 65^{o}C.

Figure 2.8 | Oxygen plasma chamber used to seal the PDMS structures to a glass slide.
The final step of the microfabrication comprises the sealing of the PDMS structures obtained within glass slides, a process accomplished with resource to an oxygen plasma system.

2.3. Slide Migration Assays

Primary biological assays were conducted with resource to standard slide experiments, aiming to validate the migration stimuli hypothesis and forecast the systems behaviour before exploring the microfluidic approach. The protocol developed comprised a set of sequential routines, including FN coating, 37ºC incubation, cell extraction for slide loading and the stimuli introduction, as summarised in Figure 2.9.

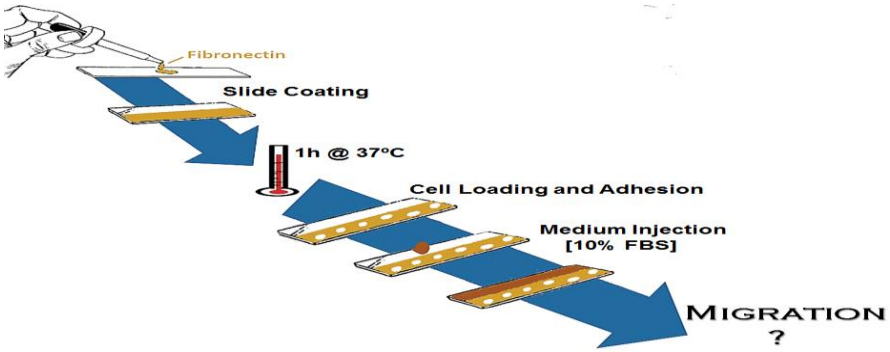

Figure 2.9 | Sequential steps comprised in the development of slide migration assays.
The experiment comprises the slide coating with FN, incubation for 37ºC, cell line preparation and loading and, ultimately, the insertion of a stimuli that is expected to promote migration.

On behalf of fibronectin coating, a volume of 80*µL* (10 $\frac{\mu g}{mL}$) fibronectin solution (Sigma) was poured into the cell plate and incubated for one hour at 37*ºC* without agitation. The fibronectin solution was then removed and the plate was ultimately washed with DPBS solution. Posteriorly, pre-trypsinized cells were loaded onto the inferior half of the slide and, after cell adhesion became evident, the stimuli was introduced – injection of an increased serum medium (89% (v/v) DMEM, 10% (v/v) FBS and 1% (v/v) PS). It is important to refer the need to submit the cells to a lower serum concentration when introducing them in the system, as described in Section 2.1.2.

Furthermore, and taking into account MEFs' specifications and optimal conditions, emerged a need to create a micro-environment with regulated temperature at approximately 37*ºC*. The platform was developed with resource to a stainless steel stage of $159 * 109 * 2\ cm^3$ containing two 17*W* power resistances and coupled to the microscope structure. The fabricated platform was then calibrated through sequential registries of temperature towards voltage until the desired 37*ºC* degrees were achieved. The results acquired are resumed on Supplementary Information (S1) through a calibration ramp from room temperatures of 25*ºC*. The final setup of the assembly engaged during a slide experiment is displayed on Fig.2.10.

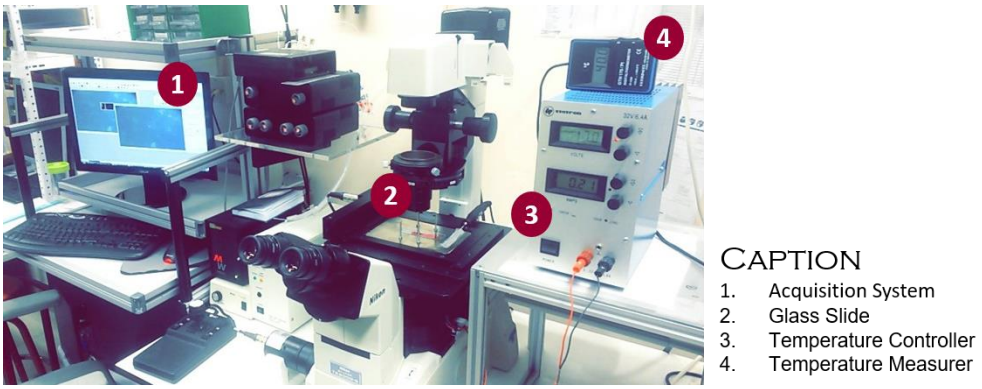

Figure 2.10 | Experimental setup of the assembly used to proceed the slide primary migration assays.
Slide assays were developed under continuous microscopic observation within a temperature controlled platform regulated through a voltage supply.

2.4. On-Chip: Migration Assays

The final biological assays were performed with resource to a microfluidic system, comprising the microdevice itself and the entire structure involved in the course of the experiment. In this context, the temperature control platform and a syringe pump were coupled to the system in order to simplify the handling of the device and optimize the protocol. The setup of the complete assembly used in this project is displayed on Fig. 2.11.

CAPTION

1. Acquisition System
2. Pressure System
3. Microchip in the heating platform
4. Syringe Pump
5. Temperature Controller
6. Temperature Measurer

Figure 2.11 | Display of the complete microfluidic assembly used in the course of migration experiments.

Experimental Protocol

The biological assays' protocol was initiated with the cleaning of the microdevices in a routine comprising the sequential use of ethanol and PBS. The fluidic block was then connected to a pneumatic pressure supplier through the inlets and outlets and the pressure was controlled through the employment of LabView Software, allowing the samples to flow along the channels.

After the assembly of the platform, a volume of 10-15*μL* fibronectin ($10\ \frac{\mu g}{mL}$) was injected in the chip and left at 37ºC during a minimum period of 1 hour. The cells were then inoculated into the microchips within a medium solution with 98% (v/v) DMEM supplemented with 1% (v/v) FBS and 1% (v/v) PS. At this point, the cells were individually separated and imprisoned by dedicated traps, bearing in mind the aim of a single-cell study. After cell adhesion was confirmed, a solution containing an increased serum level (89% (v/v) DMEM, 10% (v/v) FBS and 1% (v/v) PS) was injected in the chamber through the remaining inlets and the flow was progressively reduced in order to allow the formation of a chemical gradient within the device. Once again, it is important to refer that the cell culture must be handled in parallel with the microfluidic assembly – trypsinization and adaptation to starvation - to prevent viability losses.

The MEFs' behaviour and response to the stimuli was then followed in real time through optical microscopy and the results were recorded using the Image ProPlus Software. A general display of the assays' dynamics after the cleaning and FN incubation is presented in Fig.2.12 for a general microdevice – the protocol was then adapted to the several chips in use.

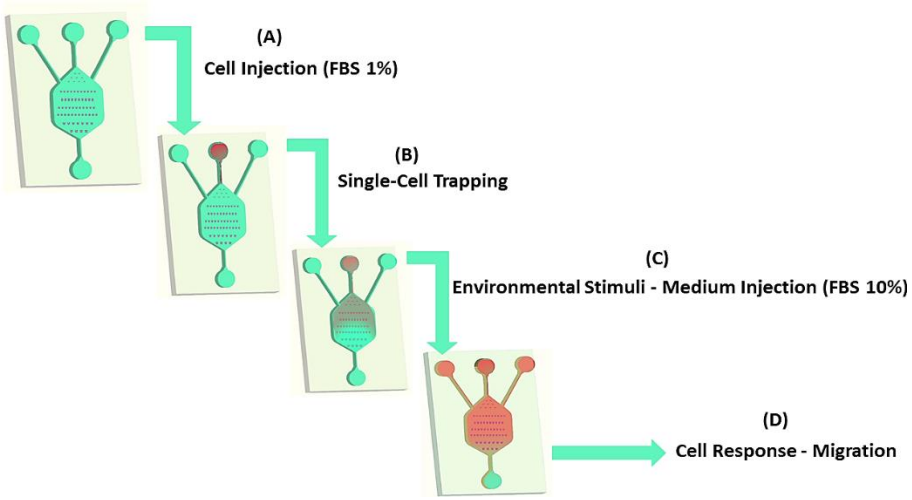

Figure 11.12 | Overall display of a generic microchip along the migration experiments.
The experiment started with the injection of a cell solution with a serum level of 1% (A). The cells were then imprisoned in the traps inside the chamber (B) and, after cell adherence, a stimuli was applied to the system through the injection of fresh medium with a serum level of 10% (C). At last, the fluid flow was interrupted and the cell response to the chemical gradient was trailed through motility tracking (D).

Chapter 3
RESULTS AND DISCUSSION

3.1. Cell Line Culture

Routines comprising the cell line development and adaptation were carefully monitored and registered, bearing in mind that the cells have a central role within the course of the proposed study. In this context, cell growing was followed every 2 days until passage for confluency evaluation and counting after trypsinization (Fig.3.1.).

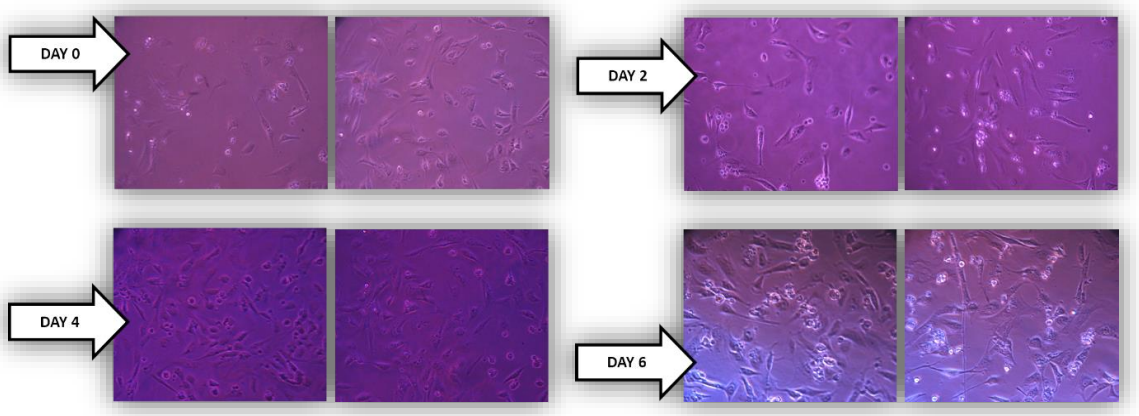

Figure 3.1 | Cell confluency from plating day (day 0) until trypsinization.
The confluency was followed every two days until an approximate value of 70%, when MEFs passaging is recommended (20x objective).

Cell trypsinization was required before each assay, since this routine allows adherent MEFs to become in suspension within culture medium. This process was found possible within a period of approximately six days since thawing, i.e., cells in culture were ready for passaging after two or three medium exchanges. First attempts of trypsinization were not successful due to the fact that the recommended incubation after trypsin was not enough to de-attach the cells from the substrate. A review of the protocol led to the value mentioned in section 2.1.1, that has made possible to remove MEFs from the well and, according to the expected, microscopic observation revealed a round-shape in the recently suspended cells (Fig.3.2.A).

Subsequent plating was performed after haemocytometer count and according to the table S2 (on Supplementary Information). In order to predict the diameter of a single MEF, a group of trypsinized cells was evaluated in terms of size. The results were acquired through the assessment of 150 generic cells with resource to ImageJ Software (Fig.3.2.B). The cells area was measured and, assuming a spherical shape, the average diameter and respective standard deviation was determined.

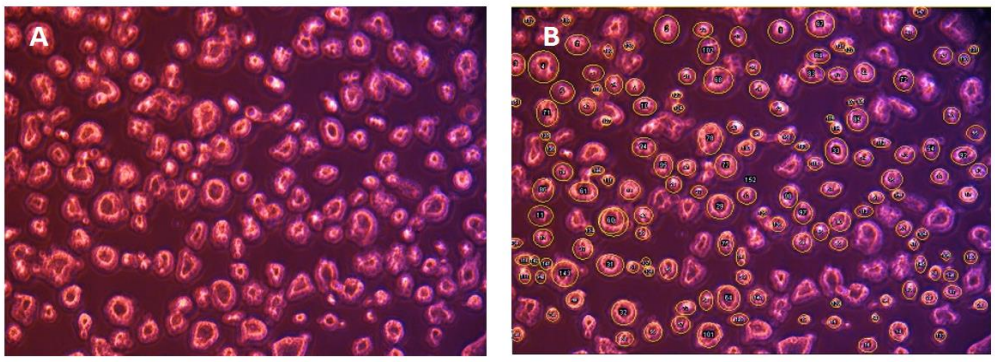

Figure 3.2 | A: Mouse Embryonic Fibroblasts in suspension exhibiting a characteristic round shape after trypsinization. B: ImageJ display wit the selection of the cells chosen to average diameter determination(20x objective).

Statistical evaluation led to an average diameter of $43.96 \pm 14{,}18\ \mu m$, according to the values extracted from ImageJ and resumed in Table S2. The distribution study – Table 3.1- revealed a Gaussian Distribution, as described in Fig.3.3.

Table 3.1 | Parameters used to determine the distribution of cell diameter after trypsinizayion in a sample containing 150 MEFs (μ=43.96*μm*, σ=14.18 *μm*).

Size Class (*μm*)	x_i	Number of Cells	f_r	Z_i	G_i
15-20	17,50	4	0,026667	-1,86552	0,000152
20-25	22,50	9	0,06	-1,51303	0,000165
25-30	27,50	13	0,086667	-1,16054	0,000179
30-35	32,50	15	0,1	-0,80805	0,000193
35-40	37,50	22	0,146667	-0,45556	0,000209
40-45	42,50	23	0,153333	-0,10307	0,000226
45-50	47,50	19	0,126667	0,249416	0,000244
50-55	52,50	12	0,08	0,601905	0,000263
55-60	57,50	9	0,06	0,954394	0,000284
60-65	62,50	9	0,06	1,306882	0,000306
65-70	67,50	8	0,053333	1,659371	0,000329
70-75	72,50	4	0,026667	2,01186	0,000355
75-80	77,50	2	0,013333	2,364349	0,000382
80-85	82,50	1	0,006667	2,716837	0,00041

The distribution, exhibiting an inferior limit of 19.15*μm* and superior of 85.85*μm* was performed considering classes of 5μm intervals. Regarding Table 3.1., X_i refers to the median value of the class, f_r the relative frequency of the occurrence, Z_i the standardized value and G_i the correspondence within the Gaussian distribution.

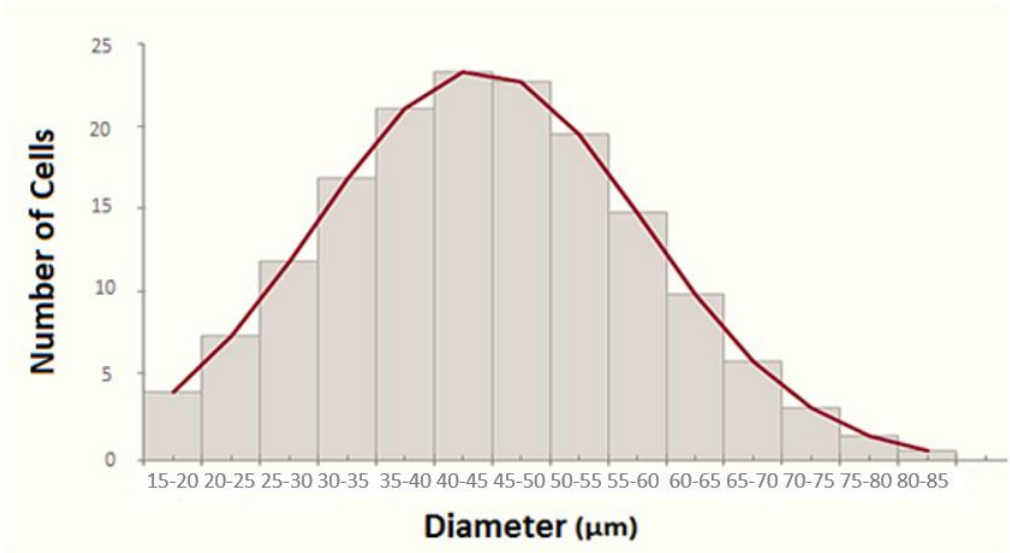

Figure 3.3 | Distribution of MEFs diameters within a sample of 150 cells (μ=43.96*μm*, σ=14.18 *μm*). MEFs diameters were obtained through ImageJ measurements of area and statistically analysed in terms of distribution, revealing a Gaussian shape.

Cell Counting Through Haemocytometer

Cell counting management along the cell line development was found suitable with a dilution factor (DF) of 2 – 20*μL* suspension cells and 20*μL* of trypan blue. A general evaluation comprising the assessment of two squares of the hemocytometer acquired in the course of cell line development is presented below (Fig.3.4.).

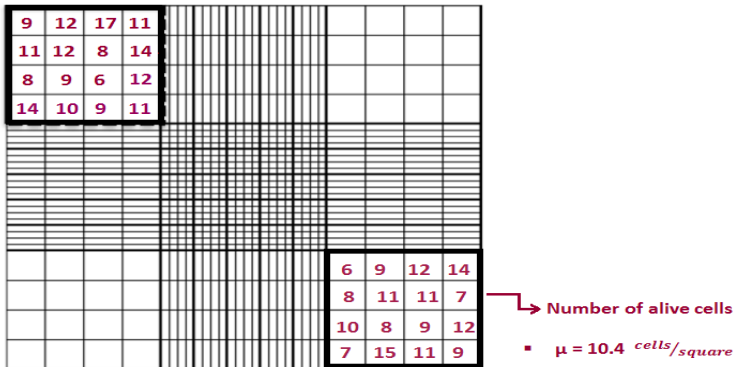

Figure 3.4 | Resume of hemocytometer counting of a MEF culture after well trypsinization.

Considering the volume of each hemocytometer square to be $10^{-4}mL$, cell concentration was determined with resource to Equation 3.1., leading to a value of $20.8 * 10^5 \ cells/_{mL}$.

$$Cell\ Concentration = \frac{N}{f} * DF * c = 20.8 * 10^5 \frac{cells}{mL} \quad \textbf{Equation (3.1.)}$$

,where *N* represents the average cell number per square counted, *f* the number of fields counted, *DF* the dilution factor and *c* the hemocytometer constant.

The Contamination Threat

Contamination is one of the main concerns when developing a cell culture, once it can lead to adverse effects on the cells, inaccurate experimental results and, obviously, loss of time, resources and money. During one of the attempts of cell line development, contamination was observed in the medium flask. As standard procedure, the contaminant was recognised as a fungi and tested in Malt Extract Agar (MEA) petri dishes for genus and species identification (Fig.3.5.). C2C1 – an ionic liquid - was used to inactivate fungal growth and a sample was prepared to microscopic examination. The fungi was identified as a *Penicillium expansum,* according to structural and morphological characteristics analysed through a dichotomous key.

Figure 3.5 | Fungi contamination emergent on the Mouse Embryonic Fibroblast culture in MEA petri dishes for genus and species identification.
The contamination found within the culture was analysed through a standard dichotomous key, leading to the identification of the sample as a *Penicillium expansum.*

3.2. Preliminary Results

As priorly mentioned, several studies were developed in order to optimize the chips performance before initiating the biological assays. In this context, preliminary results were obtained through COMSOL simulations and analysis of formerly designed trapping structures. Aiming to optimize the single-cell trapping, general tests were performed on-chip to identify the most efficient trap designs. This experiments were made using 6*μm* microbeads and allowed the assessment of the structures displayed on Fig.3.6.

Figure 3.6 | Design of the traps submitted to a performance evaluation with the use of microbeads.
The traps (A) to (F) were tested on-chip and the ones presenting a better performance were applied to the final chips to conduct the biological assays.

The process was conducted according to the procedure described on section 2.4., but at room temperature. At this point, the temperature control was not considered relevant due to the fact that the trial microbeads' functioning is not affected by this parameter. The experiment was done with resource to a pre-fabricated chip containing the 6 structures in analysis (Fig.3.7.) and each

The results (Table 3.2.) allowed a selection of the better trapping structures, which were posteriorly applied in the design of the novel chips for the migration assays. According to the trials, chips A to D were the ones presenting a higher performance, with a highlight to structures A and D. This result was in accordance with the provisions, considering the fluid tends to flow along regions with lower resistance. Due to this fact, these were the traps chosen to fabricate the chips for the development of the final assay.

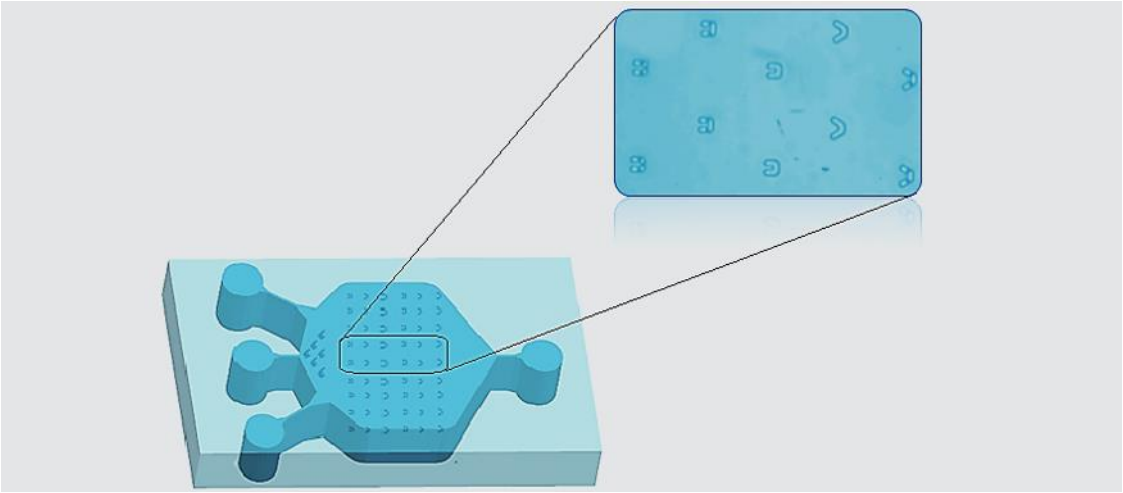

Figure 3.7 | Microchip used to study trap's efficiency and detail of the live image of the chip during the assays.
A pre-fabricated device was used to assess the best structures to capture cells with resource to microbeads.

Table 3.2 | Trapping efficiency of the pre-designed structures obtained through experiments with microbeads
Structures containing a line of flow exhibited higher rate of success and were applied in the final devices.

	Structures	Captured Particles	Efficiency (%)
Trap A	84	70	83 %
Trap B	88	61	71 %
Trap C	84	54	64 %
Trap D	84	74	88 %
Trap E	84	26	27%
Trap F	88	27	31%

Moreover, it was observed that structures (traps, chambers, channels) containing right-angles showed increased probability of bubble formation – Figure 3.8. – suggesting the application of round edges in all the finishing of the new devices projected. Alternative treatment on behalf of the bubble formation consists on cleaning the device with a surfactant as Tween or Polyethylene Glycol (PEG) before the utilization, nonetheless this procedure was not applied on the migration assays since these reagents decrease the protein adhesion to the substrate and would interfere with the Fibronectin coating process.

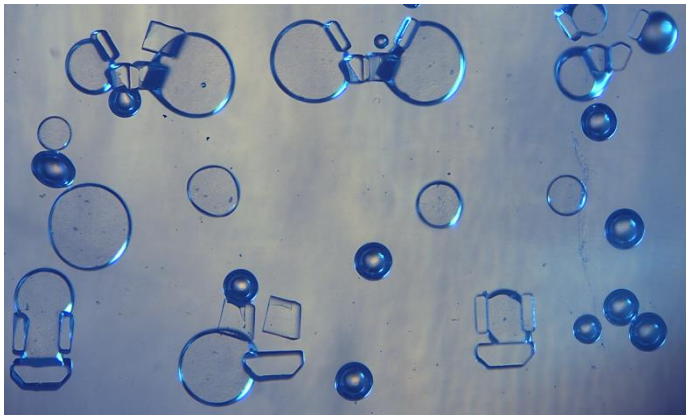

Figure 3.8 | Emmergence of bubbles during microfluidic preliminary assays due to the right-angles in the traps borders.

3.3. Chip Design and Modelling

3.3.1. Device Design

The final structure of the microfluidic chips, acquired with resource to AutoCAD, was developed considering the aim of the experimental assays and taking into account the illations from sections 3.1 and 3.2. In this context, the imprisonment of single cells through trapping structures was found suitable as a strategy to study heterogeneous cultures from an individual perspective. Therefore, the dimensioning of the traps, displayed in Fig.3.9, was projected in order to allow the imprisonment of a *Mouse Embryonic Fibroblast* and likewise considering the specifications of the microfabrication precision.

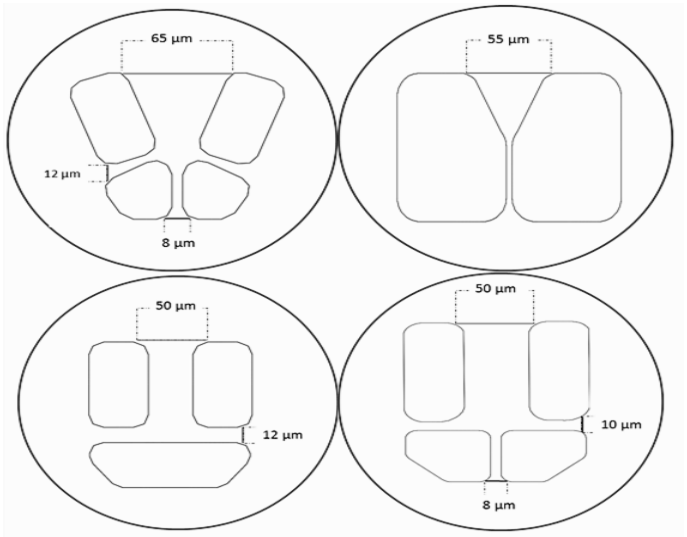

Figure 3.9 | Dimensions of the specific traping structures used in the microfluidic assays.
The traps were designed to allow a single-cell study within the migration process of MEFs and geometrically placed along the chamber device.

Moreover, and considering cell migration, new structures were introduced in order to allow cell dislocation in a channel. These structures were incorporated in four of the definitive devices, functioning simultaneously as trapping assemblies and motility passages (Fig.3.10).

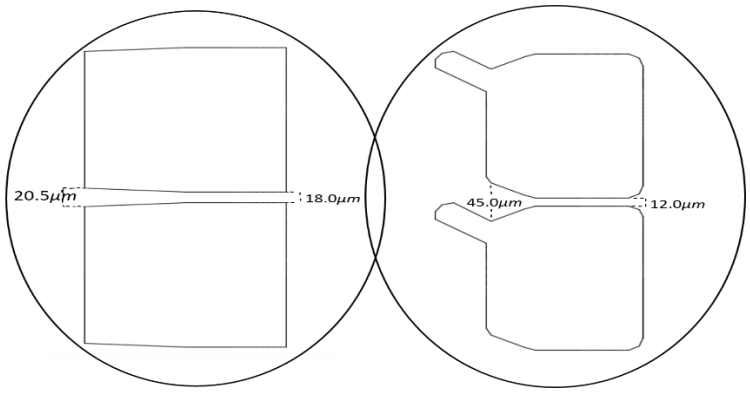

Figure 3.10 | Display and dimmensioning of the traps comprised in the device walls.

In respect to the fluidic devices *per se*, seven different chips were projected in order to entirely encompass the purposes of the analysis. In view of Fig.3.11, the structures were acquired through the development of diverse layers, distinguishing the device channels and reservoirs (in red) and the fluidic traps (in black).

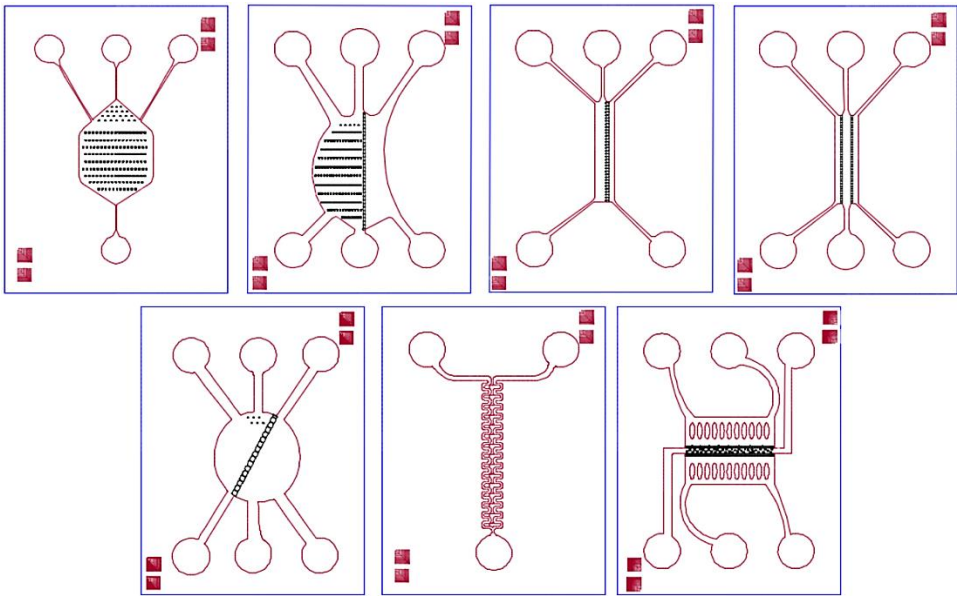

Figure 3.11 | Final schematic of the chips' design conceived for the migration assays (AutoCAD 2015).
The design of the microfluidic devices was conducted with resource to AutoCAD Software and optimized until the version presented above.

The step between the final designing and the fabrication comprised the statement of the polarization of the structures within the devices (Fig.3.12), to allow the fabrication of a mask that was posteriorly used to transfer the patterning into the silicon wafer through UV-Radiation (as illustrated in Fig.2.3).

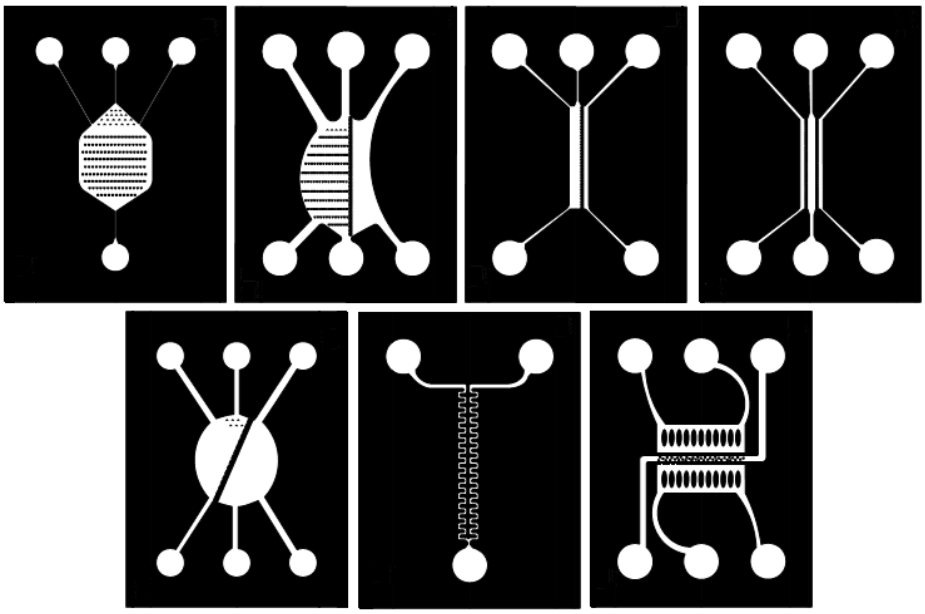

Figure 3.12 | Definition of the polarization of the fluidic devices, preceeding the mask fabrication to apply in the microfabrication process.
The designs acquired through AutoCAD were classified according to the specific polarity in order to allow the fabrication of the mask used to the patterning transference under UV-Radiation.

3.3.2. Device Modelling

The optimization of the devices was a fundamental step for the acquisition of functional platforms, comprising contemplations of fluids' behaviour, particle trajectory, chemical gradient formation and structures dimensions and distribution within the chips. The interface of the software applied for this purpose is presented on Fig.3.13, as a preview of the process.

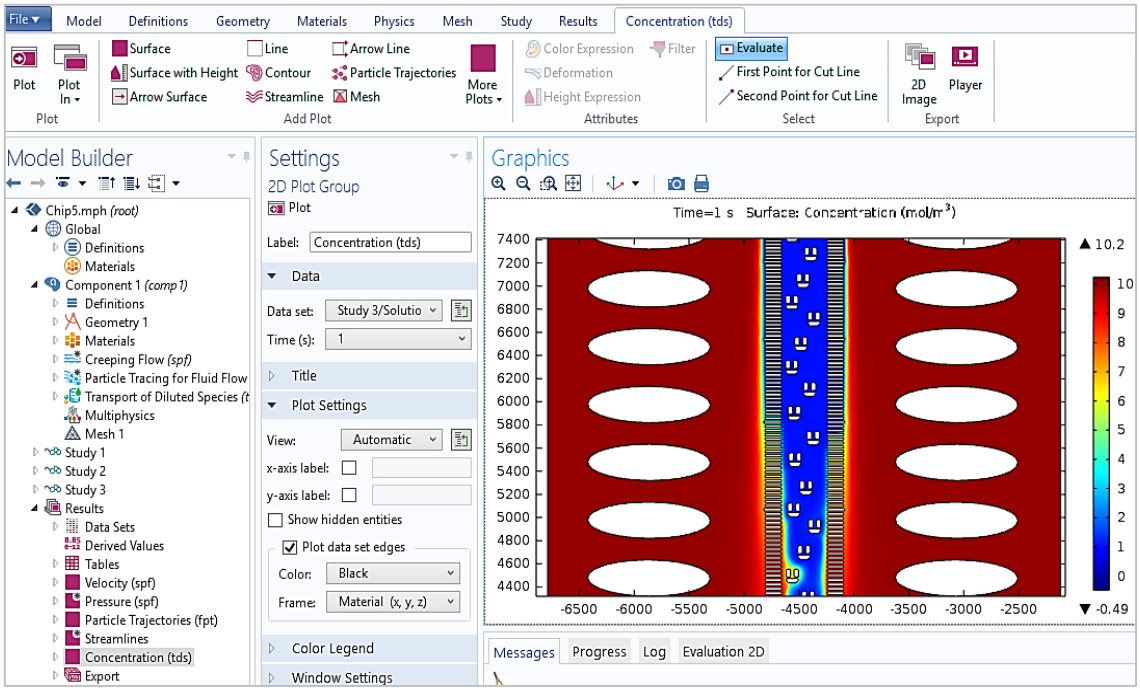

Figure 3.13 | Display of Comsol-Multyphisics 5.0 Interface during a generic study of the chemical concentration profile in a fluidic chamber.

Along this section, the results are presented for each microdevice, since the modelling was individually performed to contemplate the specifications of every device. The data was acquired through coarse meshing into two-dimensional models, in order to meet the requirements of the computational means.

Chip Number 1

This device was projected with the purpose of studying the efficiency of cells imprisonment, therefore the most relevant aspect considered was the particle trajectory. In this context, the results presented only comprise the Particle Trajectory Profile, even though other parameters were studied (data not shown).

First results showed a low trapping performance (Fig.3.14-A), leading to rearrangements of the structure to optimize the capturing of single-cells. The structural modifications included the addition of a row of flow dividers in the entrance area and a readjustment of the alignment of the traps (Fig.3.14-B). Both simulations were performed under similar conditions of pressure values, with 1.5 *kPa* for the outer inlets, 2 *kPa* for the central one (the one used to inject the cells) and 0 *kPa* for the outlet. These values were equally obtained with resource to COMSOL modelling, that led to a general conclusion that the pressure within the exterior inlets must be inferior to the one applied in the central one in order to allow a better dispersion of the fluid containing the cells and a more efficient trapping (Fig.3.15).The number of particles used to develop the trajectory profiles was 50, a value found suitable for the experiments.

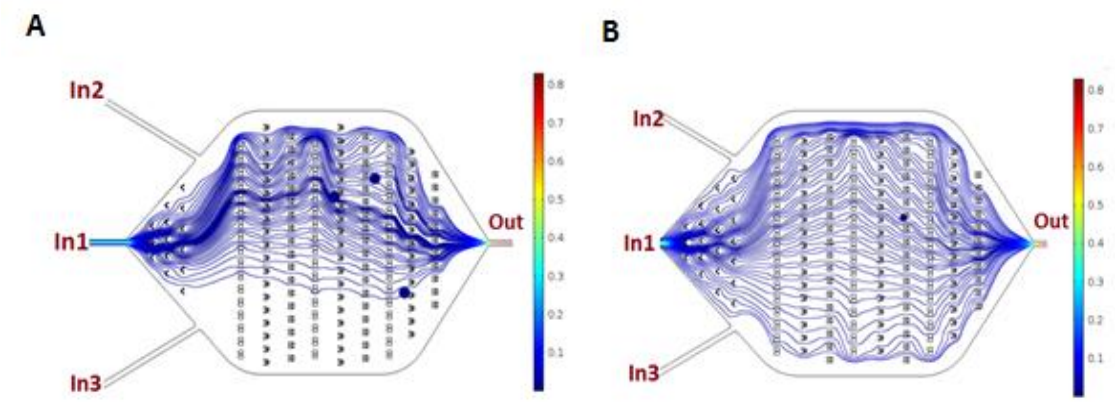

Figure 3.14 | Particle Trajectory Profiles performed to optimize trapping efficiency on Chip 1.
A: Trajectory of the particles in the primer device (N=50, P_{In1}= 2*kP*a, P_{In2} = P_{In3} = 1.5*kPa*, P_{out} = 0.0*kPa*).
B: Trajectory of the particles in the device after proper optimizing readjustments – addition of a flow dividers' row and redistribution of the traps (N=50, P_{In1}= 2.0*kPa*, P_{In2} = P_{In3} = 1.5*kPa*, P_{out} = 0.0*kPa*).

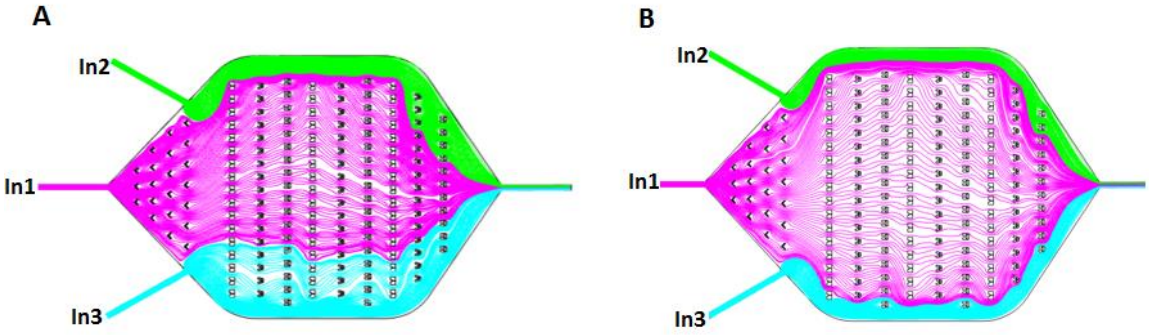

Figure 3.15 | Streamlines of Velocity Profiles applied to the device under different pressure conditions.
A: Velocity streamlines acquired for similar pressure values in all the 3 inlets (P_{In1}= P_{In2} = P_{In3} = 2.0*kPa*).
B: Velocity streamlines acquired after a pressure readjustment to promote the dispersion of the fluid containing the cells (in purple, from the central inlet) in the whole chamber (P_{In1}= 2.0*kPa*, P_{In2} = P_{In3} = 1.5*kPa*).

Chip Number 2

The purpose of this device was the evaluation of the stimulus extension, i.e., the establishment of an interval in which the cells can sense a variation in the medium concentration. Therefore, the structure includes a wall dividing the main chamber into two regions: a trapping area and an adjacent zone to allow the injection of the richest medium and a gradient formation. In this case, modelling was particularly useful to help defining the experimental parameters, such as the relative pressures of the inlets. The optimal values to operate within these device were set according to the results on Fig.3.16, which show a better deployment of the chip for a pressure value of 2*kPa* in the central inlet and 1*kPa* in the remaining. Moreover, the simulations suggested a redesign of the chip – that was initially symmetric – in order to reduce the death volume in the device chamber.

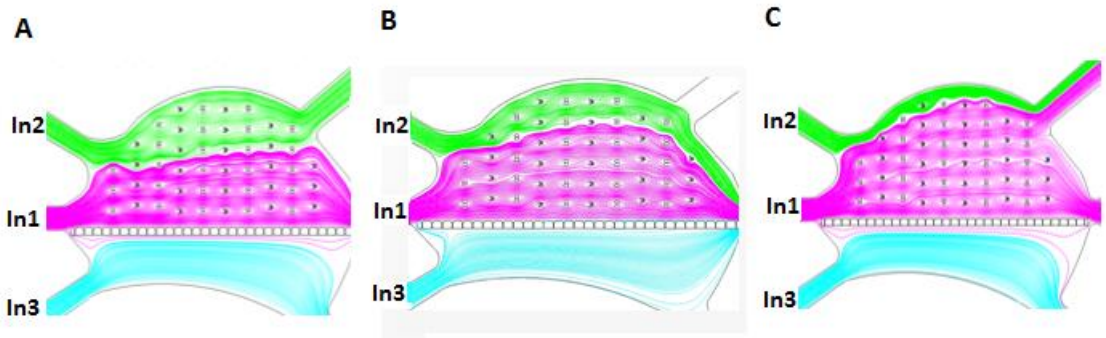

Figure 3.16 | Streamlines of Velocity Profiles developed to define the optimal pressure values for the device 2 functioning.
A: Streamlines for similar pressure values at the entrance (P_{In1}= P_{In2} = P_{In3} = 2.0*kPa*).
B: Streamlines for pressure values of P_{In1}= 2.0*kPa*, P_{In2} = P_{In3} = 1.5*kPa*.
C: Velocity streamlines acquired with P_{In1}= 2.0*kPa*, P_{In2} = P_{In3} = 1.0*kPa*.

Chip Number 3

In this case, instead of projecting a trapping region delimited by a wall, the intention was to incorporate the imprisonment structures in the wall itself (see detail in Fig.3.17). The main challenge while developing this device was the fluid control towards the trapping structures within the barrier, which requires a fine pressure control. This specific design – along with device number 6 – presents a vertical wall containing variable opening distances in order to evaluate cell elasticity, nonetheless this feature is not considerate along COMSOL simulations.

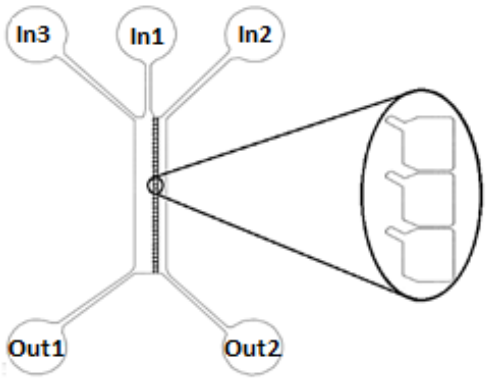

Figure 3.17 | Device in analysis, exhibiting a detail of the trapping structures in the wall dividing the chamber.

First results suggested the implementation of two outlets - instead the initial three projected -, an adjustment that led to a lower dispersion of the particles from the central region. Additionally, several Particle Trajectory and Velocity Profiles were computed to determine the ideal values of the relative pressures in the device (3.18). Taking into account the purpose of the design, the inlet pressure values were altered in order to direct the particles to the traps along the wall. Moreover, it was acknowledged that applying a small value of pressure (in the order of Pa) at Outlet 1 would benefit the flow direction as desired. The results (summarised in Fig.3.18) led to the conclusion that the more suitable parameters to the adequate functioning of the device would be 500*Pa* for inlets 1 and 2, 2*kPa* for inlet 3, 200 *Pa* for the outlet 1 and 0 at outlet 2.

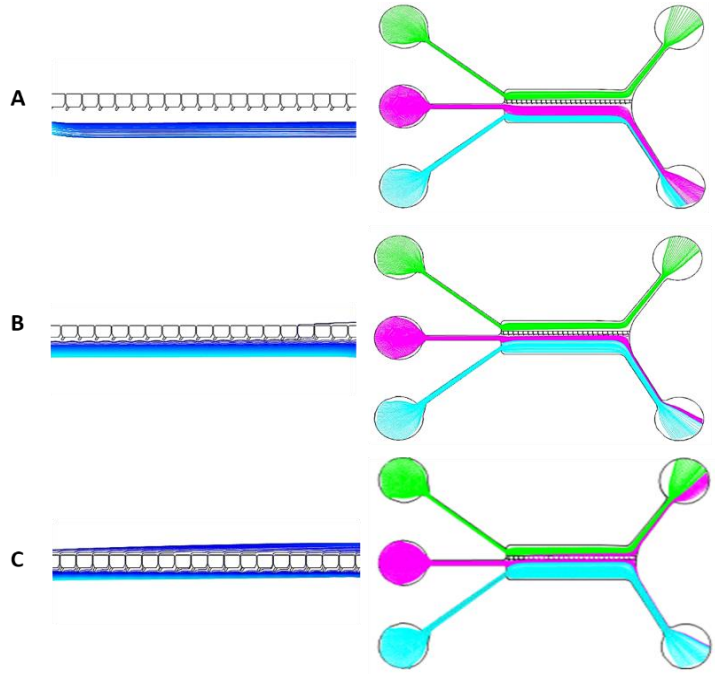

Figure 3.18 | Particle Trajectory and Velocity Streamlines Profiles acquired through pression variations in order to improve the efficiency of the device.
A: Particle Trajectory and Streamlines for similar pressure values at the entrance ($P_{In1} = P_{In2} = P_{In3} = 2.0kPa$).
B: Particle Trajectory and Streamlines for $P_{In1} = P_{In2} = 500Pa$, P_{In3}= 2kPa and $P_{out} = 0.0kPa$.
C: Particle Trajectory and Streamlines for $P_{In1} = P_{In2} = 500Pa$, $P_{In3}= 2.0kPa$, $P_{Out1} = 0.0kPa$, $P_{Out2} = 200Pa$, the preferential pressure arrangement.

Chip Number 4

This device was designed to integrate the possibility of developing a migration assay in parallel with a control test. In this context two walls containing trapping structures were projected to fit the main chamber, dividing it into three compartments, according to Figure 3.19.

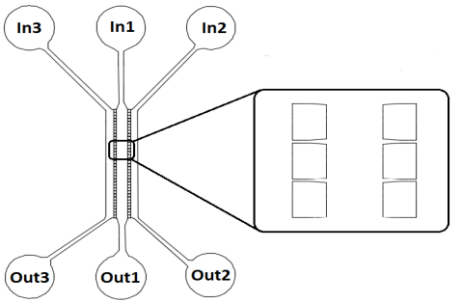

Figure 3.19 | Device display with highlight to the trapping structures inbedded in the vertical walls.

Considering the conclusions from the assessment of Device Number 3, the preferential setting was obtained for values of 2.0*kPa* at inlet 1, 500*Pa* at the remaining, 200*Pa* at outlet 1 and 0*Pa* for both outlet 2 and 3. The Particle trajectory Profile acquired for this arrangement is displayed in a close-up view on Figure 3.20.

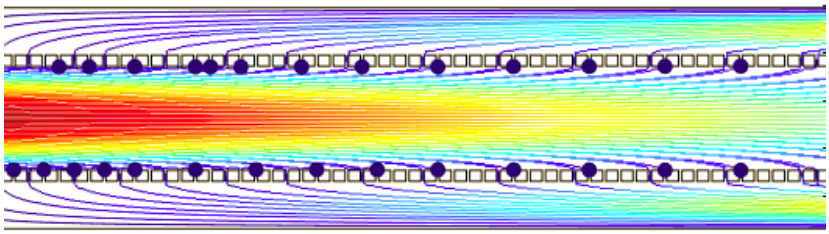

Figure 3.20 | Close-up view of the trapping obtained through a Particle Trajectory study.
Simulation of particle trajectories obtained by applying pressures of P_{In1}= 2.0*kPa*, P_{In2} = P_{In3} = 500*Pa*, P_{Out1} = 200*Pa* and P_{Out2} = P_{Out3} = 0*Pa*.

Chip Number 5

Device number 5 was equally evaluated in terms of Particle Trajectory Profiles according to the pressure values at the reservoirs. Similarly to device number 4, the objective is to have a flow barrier simultaneously working as a trapping region. Nonetheless, this geometry is expected to be easier to handle considering that the pressure control required is not so meticulous. Modelling of this device suggested a reduction in the circular chamber area (data not shown) and the optimal values of relative pressure for its functioning through consequent adaptation (Fig.3.21).

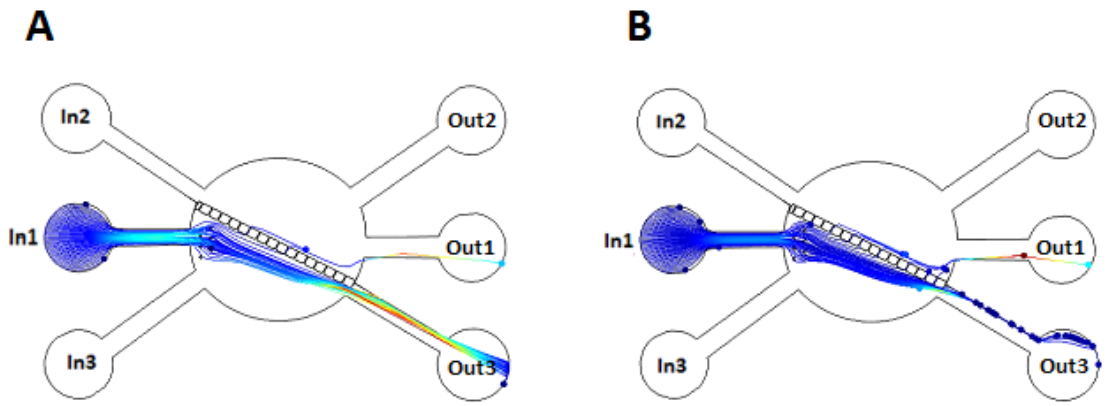

Figure 3.21 | Particle Trajectory Profiles acquired through variation of the relative pressures at the reservoirs.
A: Particle Trajectory for similar pressure values at the entrance (P_{In}= 2.0*kPa*), P_{Out1} = P_{Out2} = 0*Pa* and P_{Out1} = 1.0*kPa*. B: Particle Trajectory for similar pressure values at the entrance (P_{In}= 2.0*kPa*), P_{Out1} = P_{Out2} = 0*Pa* and P_{Out1} = 1.5*kPa*, standing as the preferential reference.

Chip Number 6

Modelling device 5 comprised, fundamentally, the optimization of the path structure and the arrangement of the trapping regions of the chip. In this case, Particle Trajectory was the preferential profile to be acquired and geometry revealed to possess manifest influence on this phenomena. Modifications of the prime design included variations in the path extension, its thickness and length and, ultimately, in the finishing of the structure - as presented on Fig.3.22.

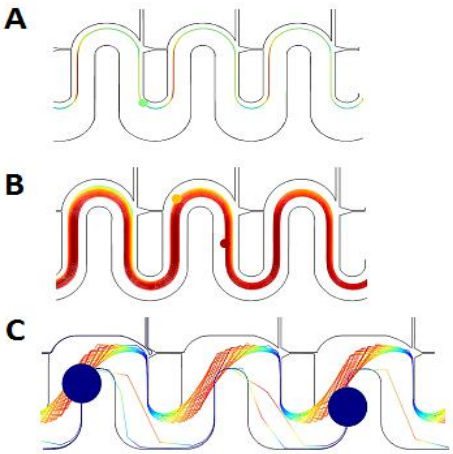

Figure 3.22 | Resume of the modifications applied in the device number 6 geometry in order to promote single-cell trapping along the channel.
Particle Trajectory was evaluated on the course of each modification, leading to the selection of the structure represented in (C).

Chip Number 7

The last device, which can also function as a control platform, has presented adequate behaviour under a generalized inlet pressure of 2*kPa* and outlet of 0*Pa* after the analysis of Velocity and Particle Trajectory Profiles.

Moreover, the diffusion of flow under continuous course was predicted considering the transport of diluted species with concentrations of 1 and 10 $\frac{mol}{m^3}$. Allowing for the unpredictability of the real concentration of species flowing in the device, this approximation was applied taking into account the variation of serum concentration in the medium, in order to obtain a preview of the gradient formation phenomena – Fig.3.23.

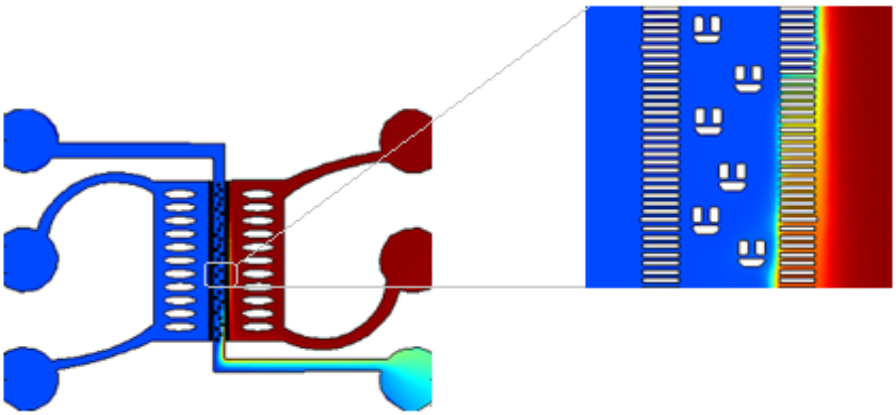

Figure 12.23 | Preview of the concentration gradient formation within the device.
The preview was obtained with resource to approximations in relation to real concentrations, since it is not possible to predict the accurate concentration of the composed fluids used during the experimental assays.

3.4. Chip Characterization

Characterization of both the SU-8 mould and the final devices was performed in CENIMAT, with resource to Cell^A Image Acquistion Software (Olympus bx51, sc30). A brief analysis of the channels/ features integrity and dimensions was performed and the fabrication parameters were reviewed in case of irregularities.

First results revealed malformations within the devices 6 and 7, exhibiting collapsed features and displacement of some structures. In relation to device number 6 (Fig.3.24), modifications included the variation of the parameters comprised in the SU-8 mould fabrication and, ultimately, a reduction in the height of the device (to 60*μm*) which is intricately related with the tolerance to produce reduced features.

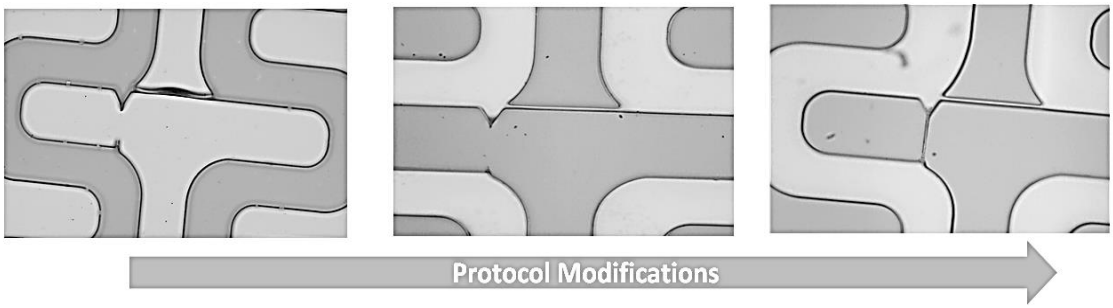

Figure 3.24 | Initial deformities found during characterization of device 6 and final accurate result after protocol modifications.
First modifications included a variation on fabrication parameters (SU-8 processing) and the optimal result was acquired towards a diminution in the height of the device and consequent protocol readjustments.

Regarding device 7, deformities appeared along the lateral channels dividing the main chamber with highlight to the zones containing the smallest separation distances (6*μm* and 8*μm*). In this case, neither protocol adjustments nor a height rearrangement were found effective and the device was considered not proficient for applying in biological assays (Fig.3.25).

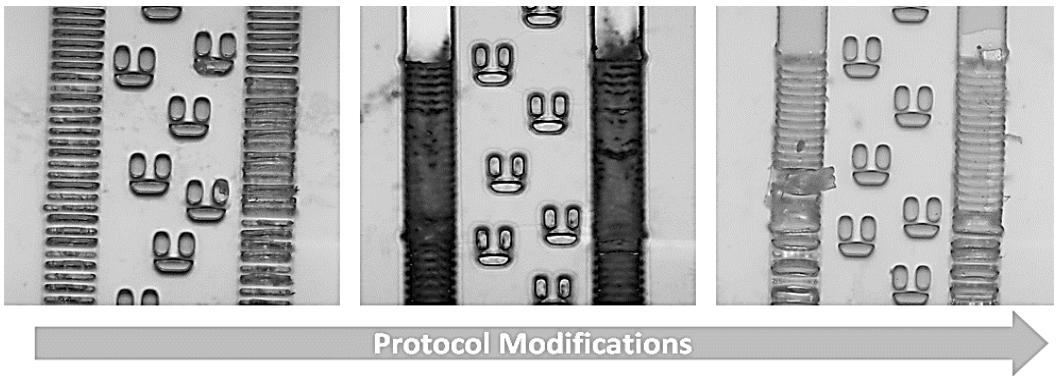

Figure 3.25 | Persistance of deformities along the channels of device 7 after protocol readjustment.
The emergent difficulties in obtaining viable devices with this features led to the exclusion of device 7 from the biological assays development.

The moulds and devices of the remaining designs were considered suitable for bio-applications after characterization and evaluation of the critical features integrity – displayed in Fig.3.26.

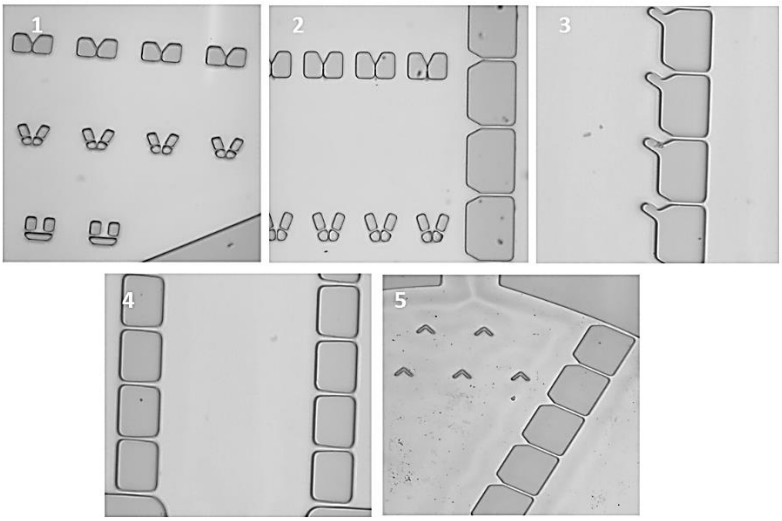

Figure 3.26 | Display of the critical features of devices 1 to 5, confirming the integrity of the structures and applicability to the bio-assays.

Moreover, the PDMS final chips were submitted to Stylus Profilometry, a common technique to measure the features height. This procedure comprised the motion of a stylus across the feature with a specific contact force, allowing the height determination according to the vertical displacement induced. The results obtained are resumed in Table 3.3., herewith correspondent average and standard deviation.

Table 3.3 | | Measurement results of features acquired through Stylus Profilometry techique and respective average and standard deviation.

Measurements (μm)	Average (μm)	Standard Deviation (μm)
78.00	**81.80**	**2.69**
80.00		
83.00		
84.00		
84.00		

3.5. Slide Primary Assays

Beforehand the development of assays comprising the appliance of microfluidic devices as a platform for a migration study, the experiment was conducted in glass slides. In this context, and in accordance with the protocol described in section 2.3., multiple hypothesis were studied in order to validate the migration phenomena and predict the course of the assays within the chips.

Assay 1 - The Employment of Fibronectin

The attachment of the fibroblasts to the substrate is the first step to be observed in the course of a migration assay. In this case, the employment of fibronectin was chosen to promote the adhesion and the effect of this protein was tested by medium injection in slides containing fibroblasts with and without fibronectin coating. The results, displayed in Fig.3.27, confirm the role of this protein towards cell adhesion to the substrate.

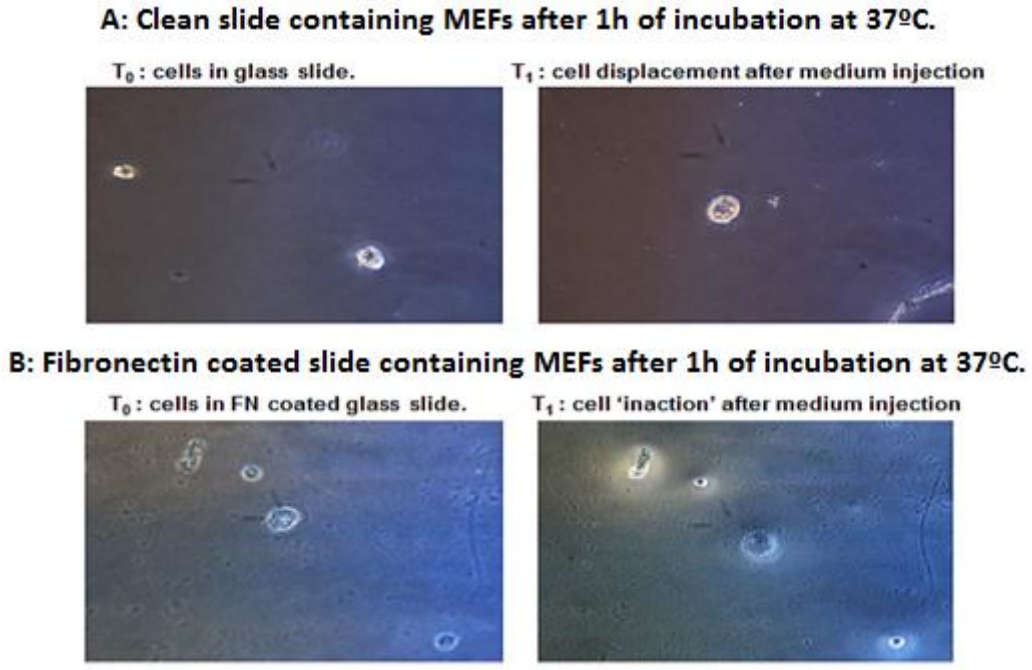

Figure 3.27 | Fundamental role of fibronectine within the cell primary adhesion to the glass substrate. Two glass slides containing mouse embryonic fibroblasts were incubated for 1*hour* at 37*ºC* and the adhesion to the substrate was tested under microscopic observation (20x objective). A: control slide without fibronectin before and after culture medium injection; B: fibronectin coated slide before and after culture medium injection.

Cells incubated within clean slides were still in suspension after 1*h* and were displaced after fresh medium injection (Fig.3.27.A), whereas the ones within FN coated slides showed motion resistance in the same conditions due to the adhesion to the substrate (Fig.3.27.B), evidencing fibronectine as an adhesion promoter.

Assay 2 – Migration Validation: the stimuli effect

To verify whether the concentration variation of the culture medium works as an environmental stimuli to trigger adherent fibroblasts migration towards the region with richer serum, a concentration gradient was applied in fibronectin coated glasses. The already adherent cells were tracked for motility during a period of 80 *minutes* and effective migration was observed (Fig.3.28.) in the direction of the stimuli.

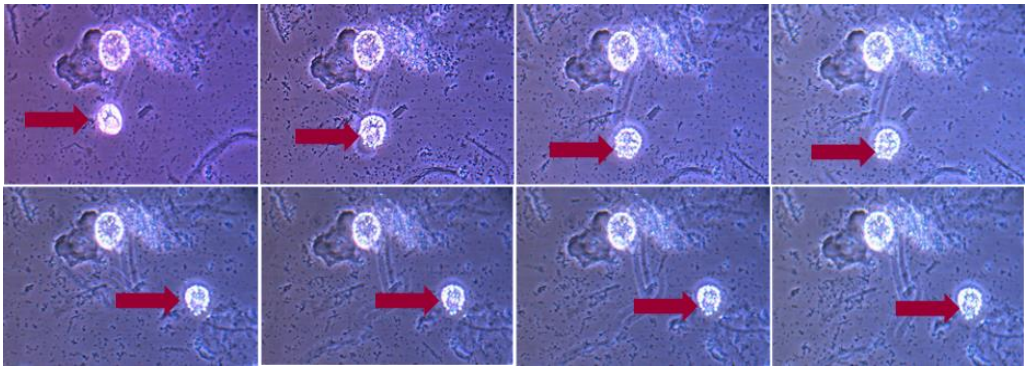

Figure 3.28 | Display of the migration sequence acquired during experimental slide assays in 10 minutes intervals.
Once cell adhesion to the slide was confirmed, the richer serum medium – working as a stimuli – was inserted and the cells migration towards it was tracked under microscope observation (20*x*).

Continuous observation led to the conclusion that cells trapped in medium residues or air dust have no equal ability to migrate, vindicating the behaviour of the bottom cell in the picture above. Moreover, the characteristic morphological transformation involved in cell migration was detected (with resource to the detail on Figure 3.29. and the adhesion structures were identified. The protrusion development at the leading edge of the cell was distinguished due to the emergence of the parallel filaments constituting filopodia, as duly signed on Figure 3.29.

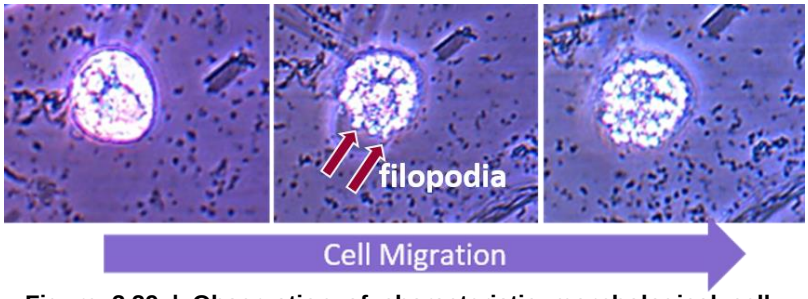

Figure 3.29 | Observation of characteristic morphological cell transformation during the migration process.

Assay 3 – Migration Control-Test: no stimuli

A control experiment comprising the insertion of a poor serum medium (1%) after the incubation of adherent MEFs to fibronectin coated slides was proceeded in order to validate the results acquired through Assay 2. In this context, the environment suffered no alteration in terms of concentration, implying the non-formation of a gradient. According to the expected, migration was not observed in the slide, reinforcing the hypothesis that the environmental alteration priory applied works as a stimuli that triggers MEFs migration. The assay, performed during 90 minutes, is resumed in Fig.3.30, through a sequence interval of 30 *minutes.*

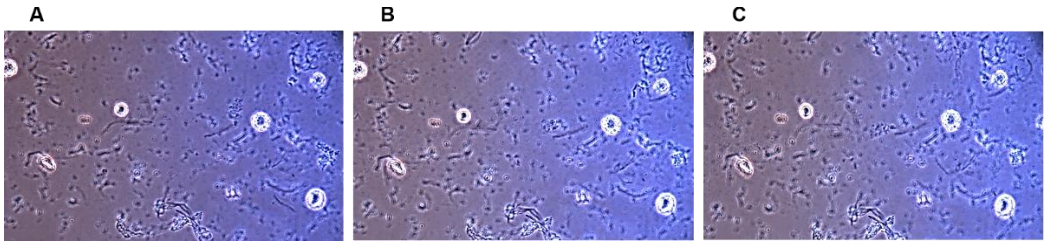

Figure 3.30 | Control-Test performed to validate the action of the pre-defined surrounding stimuli as a cell migration trigger.
The control test was performed within the same parameters of the migration assay, excluding the introduction of the stimuli in evaluation (20*x* objective).

3.6. On-Chip: Experimental Assays

Once there was experimental proof that Mouse Embryonic Fibroblasts migrate under the environmental stimuli of variating the medium concentration, new questions emerged towards the adaptation of the experiment to microfluidics: *Are the devices efficient from the trapping perspective? Is fibronectin equally effective within the chip? Will the cells adhere to the substrate? Is migration occurring?* The assays developed were conducted in order to answer this questions and, ultimately, establish whether microfluidics is a preferential method to assess migration.

3.6.1. Fibronectin Role – cell's adherence

Regarding the effect of fibronectin in the cells' adhesion, the experiment was reproduced with the same parameters as per in slide, as described in section 3.5. – Assay 1. The results were obtained by injecting culture medium in a device containing trapped cells and observing whether they showed motion to the fluids passage.

First results (comprising the insertion of the cells in a chip with no FN) have shown no adhesion efficiency after a period of 3 *hours*. Posteriorly, the repetition of the assay with a chip containing FN coating revealed effective adherence of the cells loaded approximately 1*h*30 after cell imprisonment (Fig.3.31 in 15 *minutes* interval).

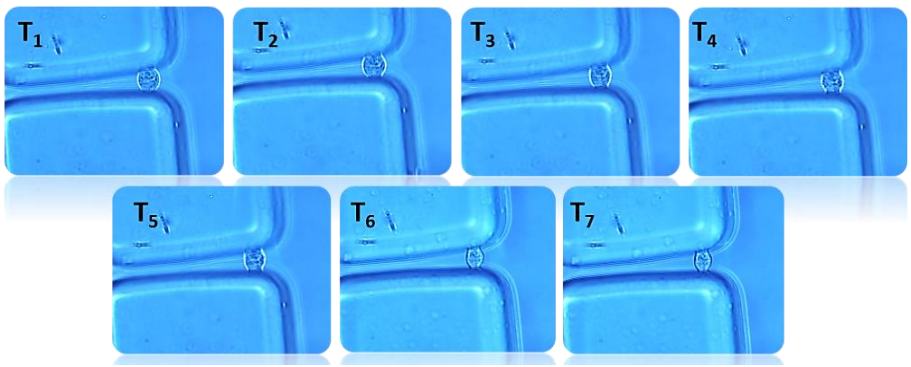

Figure 3.31 | Verification and progression of cell adhesion in a FN coated microchip.
Cell adhesion to the substrate - verified every 15 *minutes* (T_1-T7) – was confirmed 1*h*30 after cell loading and respective trapping in the device (40*x* objective).

3.6.2. Stimuli Induced Migration

The microfluidic approach applied for the migration assays comprised three sequential steps: cell trapping, cell adherence and migration-stimuli induction. It was observed no cell motility when using devices containing traps dispersed along the chamber, conceivably due to the fact that these structures worked as a barrier towards the stimuli.

On the other hand, devices containing trapping structures incorporated in walls showed efficiency and allowed the monitoring of migration along the channels. Devices 3, 4 and 7 endorsed positive results, validating the hypothesis that microfluidic chips consist on a viable tool for migration studies. The migratory sequence displayed below (Fig.3.32) was acquired with resource to device 7 during a period of 180 *minutes* (15 *minutes* interval).

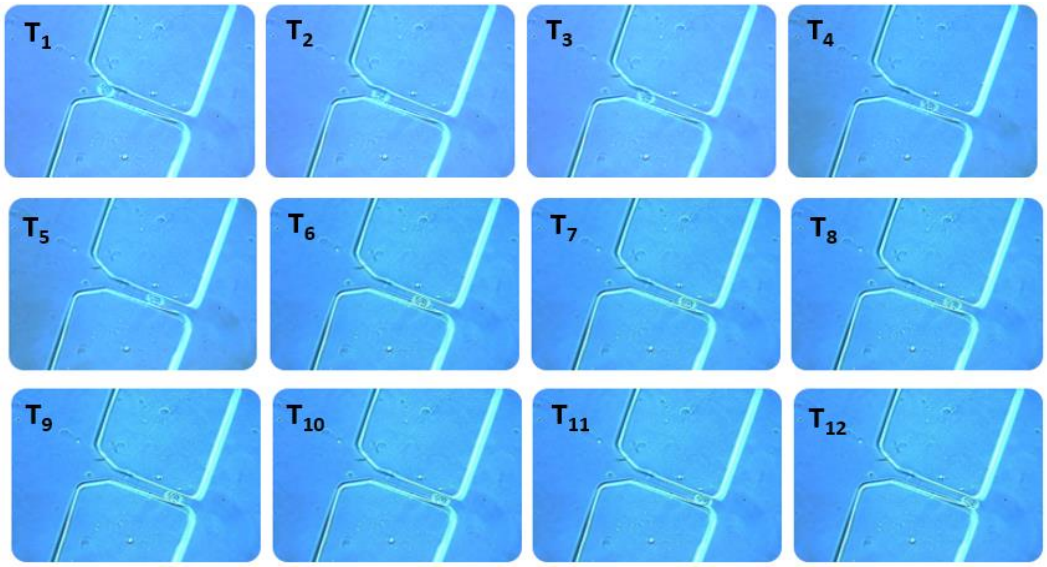

Figure 3.32 | Migration sequence through a channel (18*μm* height, 225*μm* length) during a period of 180 minutes.
Effective migration was observed and registered every 15 *minutes*, within the channels of the device towards the environmental stimuli applied (20x objective).

After the experiment was concluded (and migration was observed), data analysis led to the conclusion that the tracked cell had a diameter of approximately 41*μm*. Considering the channel possesses a height of 18*μm*, this outcome suggests a readjustment of approximately half the size of the fibroblast and a new question emerges: *Is a cytoskeleton reorganization process induced within the cell during migration towards the stimuli? What is the pliability limit of the organelles comprising the cells?*

3.6.3. Control-Test

The validation of the migration stimuli requires a negative control, i.e., the reproduction of the experiment without the formation of a concentration gradient. In this context, a parallel study was developed to verify this hypothesis, taking into account the procedures applied in the prior section. Once MEFs were considered adherent, the cells were monitored for a period 240 *minutes* and no motility was observed in the device – Fig.3.33.

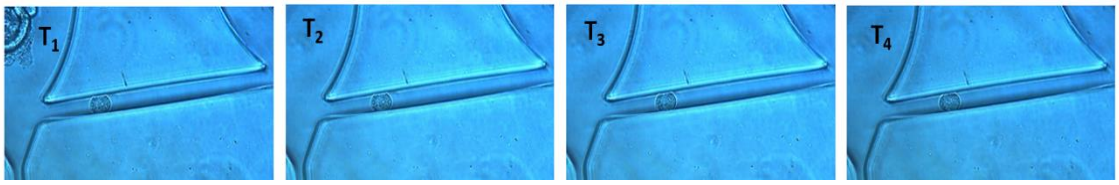

Figure 3.33 | Migration control-test: no motility was observed without the introduction of the environmental stimuli in study (20x objective).

This result led to the ultimate validation of the hypothesis established, endorsing the role of the environmental variation introduced as a trigger to MEFs migration.

CHAPTER 4
CONCLUSIONS & FUTURE PERSPECTIVES

.

WHAT WAS CONCLUDED?

The development of this project has endorsed the hypothesis that a variation on the cell surrounding environment functions as a migration trigger and allowed this phenomena assessment along its sequential stages. The stimuli introduced – a variation on culture medium concentration – was, therefore, proven successful, along with the fundamental role of fibronectin within the adhesion process. In terms of characterization, Mouse Embryonic Fibroblasts were defined as haptotactic migraters (induced by fluctuations on substrates concentration) and it was verified that cell motility occurred directionally towards the stimuli.

Primary assays, developed with resource to elementary glass slides, were particularly useful to predict the course of the experiments and optimize the pre-defined protocol applied during the migration studies. As regards the microfluidic approach, this tool has effectively substantiated its reputation as an alternative method for biological applications. Concerning this project, the employment of microdevices exhibited evident advantages in terms of the volume of reagents disposed and an enhanced response when developing protracted assays. Bearing in mind that migration occurs during a long-time period, the “encapsulation” of the experiment within a chip consisted on a visible improvement in terms of keeping the sample constantly humidified and in consistence with its natural environment.

WHAT CAN BE IMPROVED?

In terms of optimization, it would be important to improve large-scale microfabrication in order to produce appropriate standardised devices and uniform the results. Moreover, the development of a metal chip holder could substantially improve the handling of the microfluidic platform and enhance the heat transference into the microdevice. At last, more complex computational techniques (as Direct Simulation Monte Carlo) could fill out some *lacuna* towards the software employed and enable a closer approximation of the parameters to reality.

WHAT CAN BE PROSPECTED?

Regarding future perspectives, subsequent studies might include a comparative analysis of the behaviour of Mouse Embryonic Fibroblasts descendants – cells in P2, P3 – and the projection of a microfluidic device proficient for cell culture development. Additionally, it would be interesting to closely analyse the cells ability to structurally rearrange and set the pliability limit they acquire in the course of migration. Ultimately, it would be interesting to extend the biological assay developed with the aim to recover the adherent MEFs from the microchip and place them back in culture to assess its functioning and viability after the experiment.

Supplementary Information

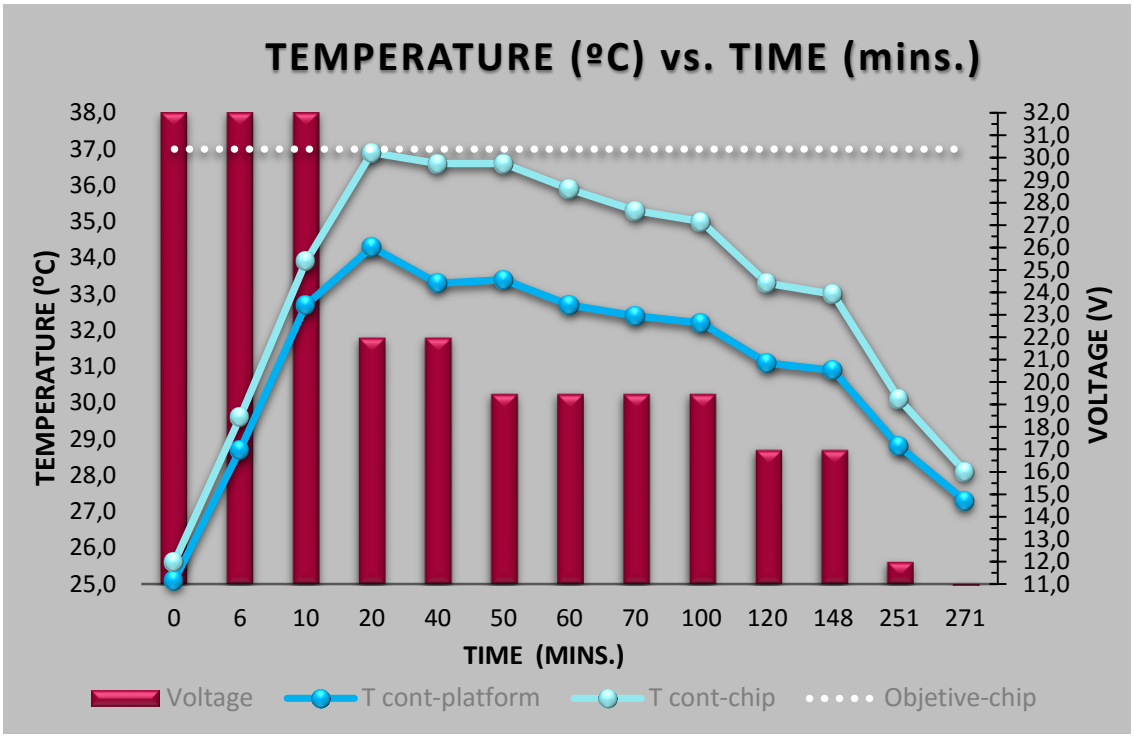

Figure S1 | Calibration ramp obtained for the temperature stabilization at 37*ºC* from an initial environmental temperature of 25*ºC*.
The calibration was obtained for variable voltage values and correspondent temperature was measured in the stainless steel platform (T cont-platform) and inside the microchips (T cont-chip).

Table S2 | Recommended plating area of Mouse Embryonic Fibroblasts according to the number of cells found in solution.
*Per well, can vary depending on the supplier. **Assuming confluent growth.

Cell Culture Vessel	Growth area (cm^2)*	No. of Cells **
Multiwell plates		
98	0.3	$4.0 – 5.0*10^4$
48	0.7	$1.3*10^5$
24	2	$2.5*10^5$
12	4	$5.0*10^5$
6	10	$1.2*10^6$
Dishes		
35*mm*	10	$1.2*10^6$
60*mm*	20	$2.5*10^6$
100*mm*	60	$7.5*10^6$
145 - 150*mm*	140	$1.8*10^7$
Flasks		
T25	25	$3.1*10^6$
T75	75	$9.4*10^6$
T150	170	$1.9*10^7$
T162	162	$2.0*10^7$
T165	165	$2.1*10^7$
40 - 50*mL*	25	$3.1*10^6$
250 - 300*mL*	75	$9.4*10^6$
650 - 750*mL*	162 – 175	$2.0*10^7$
900*mL*	225	$2.8*10^7$

Bibliography

1. Horwitz R, Webb D. Cell migration. *Curr Biol*. 13(9):756-758. doi:10.1242/jcs.02662.

2. Vicente-Manzanares M, Rick DJW and A, Horwitz. Cell migration at a glance. *J Cell Sci*. 2005:4917-4919.

3. Garfield AS. Derivation of primary mousse embryonic fibroblast (PMEF) culture.

4. Wheatley DN. Diffusion, perfusion and the exclusion principles in the structural and functional organization of the living cell: reappraisal of the properties of the “ground substance”. *J Exp Biol*. 2003;206(Pt 12):1955-1961. doi:10.1242/jeb.00238.

5. Haugsten EM, Wiedlocha A, Olsnes S, Wesche J. Roles of fibroblast growth factor receptors in carcinogenesis. *Mol Cancer Res*. 2010;8(11):1439-1452. doi:10.1158/1541-7786.MCR-10-0168.

6. Fibroblast. http://fat.surin.rmuti.ac.th/teacher/songchai/tissue web/fibroblast.htm.

7. Occleston NL, Daniels JT, Tarnuzzer RW, et al. Single exposures to antiproliferatives: Long-term effects on ocular fibroblast wound-healing behavior. *Investig Ophthalmol Vis Sci*. 1997;38(10):1998-2007.

8. Neil T. Bennett GSS. Growth factors and wound healing: Biochemical properties. *Am J Surg*. 1993:728-737.

9. L.G. Villa-Diaz , A.M. Ross, J. Lahann PHK. The Evolution of human pluripotent stem cell culture - from feeder cells to synthetic coating. *Changes*. 2012;29(6):997-1003. doi:10.1016/j.biotechadv.2011.08.021.Secreted.

10. Takahashi K, Yamanaka S. Induction of Pluripotent Stem Cells from Mouse Embryonic and Adult Fibroblast Cultures by Defined Factors. *Cell*. 2006;126(4):663-676. doi:10.1016/j.cell.2006.07.024.

11. Kurosaka S, Kashina A. Cell biology of embryonic migration. *Birth Defects Res Part C - Embryo Today Rev*. 2008;84(2):102-122. doi:10.1002/bdrc.20125.

12. Vicente-Manzanares M, Zareno J, Whitmore L, Choi CK, Horwitz AF. Regulation of protrusion, adhesion dynamics, and polarity by myosins IIA and IIB in migrating cells. *J Cell Biol*. 2007;176(5):573-580.

13. Consortium CM. Protrusion. 2014. https://www.cellmigration.org/topics/protrusion.shtml.

14. Vicente-Manzanares M, Choi CK, Horwitz AR. Integrins in cell migration--the actin connection. *J Cell Sci*. 2009;122(Pt 2):199-206. doi:10.1242/jcs.018564.

15. Vicente-Manzanares M, Koach MA, Whitmore L, Lamers ML, Horwitz AF. Segregation and activation of myosin IIB creates a rear in migrating cells. *J Cell Biol*. 2008;183(3):543-554.

16. Mseka T, Coughlin M, Cramer LP. Graded actin filament polarity is the organization of oriented actomyosin II filament bundles required for fibroblast polarization. *Cell Motil Cytoskeleton*. 2009;66(9):743-753.

17. Ladoux B, Nicolas A. Physically based principles of cell adhesion mechanosensitivity in tissues. *Reports Prog Phys*. 2012;75(11):116601. doi:10.1088/0034-4885/75/11/116601.

18. Gumbiner BM. Cell adhesion: The molecular basis of tissue architecture and morphogenesis. *Cell*. 1996;84(3):345-357.

19. Alexandrova AY, Arnold K, Schaub S, et al. Comparative dynamics of retrograde actin flow and focal adhesions: Formation of nascent adhesions triggers transition from fast to slow flow. *PLoS One*. 2008;3(9).

20. Zaidel-Bar R, Ballestrem C, Kam Z, Geiger B. Early molecular events in the assembly of matrix adhesions at the leading edge of migrating cells. *J Cell Sci*. 2003;116(Pt 22):4605-4613.

21. Zaidel-Bar R, Cohen M, Addadi L, Geiger B. Hierarchical assembly of cell-matrix adhesion complexes. *Biochem Soc Trans*. 2004;32(Pt3):416-420.

22. Huttenlocher A, Horwitz AR. Integrins in cell migration. *Cold Spring Harb Perspect Biol*. 2011;3(9):1-16.

23. Yamada KM, Geiger B. Molecular interactions in cell adhesion complexes. *Curr Opin Cell Biol*. 1997;9(1):76-85. doi:S0955-0674(97)80155-X [pii].

24. Whitesides GM. The origins and the future of microfluidics. *Nature*. 2006;442(7101):368-373. doi:10.1038/nature05058.

25. Thomas Braschler, Lynda Metref, Ronit Zvitov–Marabi, Harald van Lintel, Nicolas Demierre, Joël Theytaza PR. A simple pneumatic setup for driving microfluidics. *Lab a Chip Miniaturisation Chem physics, Biol Mater Sci Bioeng*. 2007:420-422.

26. Addae-Mensah K a., Wang Z, Parsa H, Chin SY, Laksanasopin T, Sia SK. Fundamentals of Microfluidics Devices. *Microfluid Devices Nanotechnol Fundam Concepts*. 2010:1-38. doi:10.1002/9780470622636.ch1.

27. Lindström S, Andersson-Svahn H. Miniaturization of biological assays - Overview on microwell devices for single-cell analyses. *Biochim Biophys Acta - Gen Subj*. 2011;1810(3):308-316. doi:10.1016/j.bbagen.2010.04.009.

28. Herold KE, Rasooly A. *Lab on a Chip Technology, Volume 1: Fabrication and Microfluidics*. Horizon Scientific Press; 2009.

29. Tabeling P. *Introduction to Microfluidics*. Oxford University Press; 2005.

30. Schmid A, Kortmann H, Dittrich PS, Blank LM. Chemical and biological single cell analysis. *Curr Opin Biotechnol*. 2010;21(1):12-20. doi:10.1016/j.copbio.2010.01.007.

31. Raser JM, O'Shea EK. Noise in gene expression: origins, consequences, and control. *Science*. 2005;309(5743):2010-2013.

32. Nilsson J, Evander M, Hammarström B, Laurell T. Review of cell and particle trapping in microfluidic systems. *Anal Chim Acta*. 2009;649(2):141-157. doi:10.1016/j.aca.2009.07.017.

33. Lindström S, Andersson-Svahn H. Overview of single-cell analyses: microdevices and applications. *Lab Chip*. 2010;10(24):3363-3372.

34. Lindström S, Hammond M, Brismar H, Andersson-Svahn H, Ahmadian A. PCR amplification and genetic analysis in a microwell cell culturing chip. *Lab Chip*. 2009;9(24):3465-3471.

35. Leng J, Salmon J-B. Microfluidic crystallization. *Lab Chip*. 2009;9(1):24-34.

36. Love KR, Bagh S, Choi J, Love JC. Microtools for single-cell analysis in biopharmaceutical development and manufacturing. *Trends Biotechnol*. 2013;31(5):280-286.

37. Janasek D, Franzke J, Manz A. Scaling and the design of miniaturized chemical-analysis systems. *Nature*. 2006;442(7101):374-380. http://dx.doi.org/10.1038/nature05059.

38. Reynolds O. An Experimental Investigation of the Circumstances Which Determine Whether the Motion of Water Shall Be Direct or Sinuous, and of the Law of Resistance in Parallel Channels. *Philos Trans R Soc London*. 1883;174(0):935-982.

39. Capretto L, Cheng W, Hill M, Zhang X. Micromixing within microfluidic devices. *Top Curr Chem*. 2011;304:27-68.

40. Kim, P., Kwon, K.W., Park, M.C., Lee, S.H., Kim, S.M., Suh KY. Soft Lithography for Microfluidics: a Review. *Biochip J*. 2008;2(11).

41. Mustin B, Stoeber B. *Low Cost Integration of 3D-Electrode Structures into Microfluidic Devices by Replica Molding*.; 2012. doi:10.1039/c2lc40728k.

42. Al. W et. *Microcontact Printing-Based Fabrication of Digital Microfluidic Devices.*; 2006.

43. Sugioka, K., Cheng Y. Femtosecond Laser 3D Micromachining for Microfluidic and Optofluidic ApplicationsEngineering. 2014.

44. Becker, H., Dietz, W., Dannberg P. Microfluidic manifolds by polymer hot embossing for µtas applications. In: *Proceedings of Micro Total Analysis Systems,.*; 1998:253-256.

45. Madou M. *Fundamentals of Microfabrication*.; 2002.

46. Campo a Del, Greiner C. SU-8: a photoresist for high-aspect-ratio and 3D submicron lithography. *J Micromechanics Microengineering*. 2007;17(6):R81-R95. doi:10.1088/0960-1317/17/6/R01.

47. Stroock a. D, Whitesides GM. Components for integrated poly (dimethylsiloxane) microfluidic systems. *Electrophoresis*. 2002;23(20):3461-3473. doi:10.1002/1522-2683(200210)23:20<3461::AID-ELPS3461>3.0.CO;2-8.

48. Whitesides GM, Ostuni E, Takayama S, Jiang X, Ingber DE. Soft lithography in biology and biochemistry. In: *Annu. Rev. Biomed. Eng.*Vol 3.; 2001:335-373. doi:10.1146/annurev.bioeng.3.1.335.

49. Hashim U, Rahman KA, Abdullah ARAJ. Mask design and fabrication of LiSFET for light sensor application. In: *2008 International Conference on Electronic Design, ICED 2008*.; 2008.

50. JD Photo-Tools. The Photo-Mask Guide. 2014:89. http://en.calameo.com/read/0001274256f3e90753b8a.

51. EQUIPMENT AND PROTOCOLS FOR HEATING SU-8 MOLDS. http://www.elveflow.com/microfluidic-reviews-and-tutorials/su-8-baking.

52. MicroChem (2012). SU-8 2000 Permanent Epoxy Negative Photoresist, Processing Guidelines for: SU-8 2025, SU-8 2035, SU-8 2050 and SU-8 2075. http://www.microchem.com.